Agriculture and Biology 2026, 2(2), 17–51.
https://doi.org/10.70737/k59jqk83

Article

Exogenous Trehalose Improved Wheat Yield by Enhancing the Post-Anthesis Photosynthetic Capacity of Flag Leaves

Yonghui Fan [1,†], Nan Chen [1,†], Xiang Yu [1], Ling Xu [1], Yongbo Yu [1], Yuxing Li [2], Bixin Lei [1], Xiuyu Wang [1], Wenjing Zhang [1], Shangyu Ma [1], Zhen Zhang [1], Zhuangzhuang Sun [1], Haipeng Zhang [1], Dong Jiang [1], Zhenglai Huang [1,*]

[1] College of Agronomy, Anhui Agricultural University, Key Laboratory of Wheat Biology and Genetic Improvement in South Yellow & Huai River Valley, Ministry of Agriculture, Hefei 230000, China
[2] Jiangsu Coastal Area Institute of Agricultural Sciences, Yancheng 224002, China
[*] **Corresponding author:** xdnyyjs@163.com
[†] These authors contributed equally to this work.

CITATION

Fan Y., Chen N., Yu X., Xu L., Yu Y., Li Y., Lei B., Wang X., Zhang W., Ma S., Zhang Z., Sun Z., Zhang H., Jiang D., Huang Z. Exogenous trehalose improved wheat yield by enhancing the post-anthesis photosynthetic capacity of flag leaves. Agriculture and Biology. 2026, 2(2): 17–51. https://doi.org/10.70737/k59jqk83

ARTICLE INFO

Received: 28 May 2026
Accepted: 6 August 2026
Available online: 17 August 2026

Abstract: In the Huang-Huai-Hai region, high-temperature events frequently occur during the grain-filling stage, posing an increasing threat to winter wheat yield. Heat stress accelerates flag-leaf senescence and impairs post-anthesis photosynthesis, thereby limiting assimilate supply for grain filling. A two-year field experiment was conducted using the heat-tolerant cultivar ‘Huaimai 33’ (HM33) and the heat-sensitive cultivar ‘Fanmai 5’ (FM5). Trehalose (TRE) at 10, 15, and 20 mmol L^{-1} was foliar-applied at anthesis, and passive warming was imposed from 15 days after anthesis for 5 consecutive days during grain filling. Grain yield, dry matter accumulation and allocation, flag-leaf photosynthetic characteristics, chlorophyll fluorescence, and sugar-related traits were determined. Heat stress markedly reduced grain yield and flag-leaf photosynthetic performance in both cultivars, with FM5 showing greater sensitivity than HM33. Among the TRE treatments, 15 mmol L^{-1} TRE showed the greatest effect. Compared with the heat-stress treatment, 15 mmol L^{-1} TRE increased grain yield by 5.40%–7.04% in HM33 and by 6.43%–9.76% in FM5 across the two growing seasons, mainly through increasing thousand-grain weight. At 21 days after anthesis, this treatment increased the net photosynthetic rate of flag leaves by 12.97% in HM33 and 19.08% in FM5. It also increased the proportion of dry matter allocated to grains at maturity from 42.56% to 46.28% in HM33 and from 43.86% to 48.42% in FM5. These results indicate that foliar application of 15 mmol L^{-1} TRE alleviates terminal heat-induced yield loss by maintaining post-anthesis flag-leaf photosynthetic capacity and promoting assimilate allocation to grains. TRE application may provide a practical approach for improving wheat heat resilience during grain filling.

Keywords: trehalose; wheat; high temperature during grain filling; yield; photosynthesis

1. Introduction

Wheat is a major staple crop in China, and winter wheat production in the Huang-Huai-Hai region is important for national food security [1] (pp. 44–52). However, frequent high-temperature events during the grain-filling period have severely constrained wheat yield in this region [1,2] (pp. 44–52). To alleviate the adverse effects of heat stress, the application of exogenous compounds to enhance plant heat tolerance has emerged as a practical and promising strategy [3] (pp. 99–106). For example, potassium dihydrogen phosphate (KH_2PO_4) and nitric oxide (NO) have been used to alleviate heat-induced injury in wheat [2,4].

TRE is highly hydrophilic and has a strong water-holding capacity, and its endogenous content has been reported to increase significantly under stress conditions [5,6] (pp. 265–274, pp. 1817–1826). Previous studies have shown that TRE can protect biomembrane systems and proteins in rice from high-temperature damage [7] (pp. 15898–15903). In wheat, exogenous TRE has also been reported to alleviate drought and heat stress by modulating antioxidant defense systems and osmotic balance [8]. However, previous studies on TRE in wheat have predominantly focused on the seedling stage or general physiological responses. The precise mechanisms by which exogenous TRE regulates post-anthesis source-sink relationships, sugar partitioning, and grain-filling dynamics under terminal heat stress remain poorly understood.

Wheat yield is primarily determined by three major components: spike number, grain number per spike, and thousand-grain weight. Among these components, grain filling is a critical developmental process that ultimately determines final yield [9] (pp. 2083). However, this pivotal stage is highly susceptible to elevated temperature. High-temperature stress during anthesis and grain filling can impair wheat growth and development, thereby reducing both grain yield and quality [10] (pp. 1). Heat stress during the mid-grain-filling stage has been reported to cause greater yield losses than stress occurring at other developmental stages [11] (pp. 739–749). Consistent with this stage-specific sensitivity, heat stress during mid-to-late grain filling results in greater reductions in grain number per spike, grain weight, and yield than heat stress during early grain filling [12]. The magnitude of heat-induced yield loss is further modulated by genotypic differences in heat tolerance [13,14] (pp. 1783–1795). In this context, post-anthesis heat stress reduces thousand-grain weight, grain-filling rate, and grain-filling duration, ultimately decreasing final grain weight and seed yield [15,16] (pp. 103408, pp. 335–344). This effect is particularly severe during the mid-to-late grain-filling stage, when heat stress further reduces grain-filling rate, thousand-grain weight, and overall yield under field conditions [17] (pp. 1239–1245). Moreover, heat responses vary among genotypes: heat-tolerant cultivars are mainly affected at 30 days after anthesis, whereas heat-sensitive cultivars show reduced grain-filling rates as early as the rapid grain-filling stage [18] (pp. 747). Consequently, recurrent heat events in the Huang-Huai wheat region of China cause yield losses of 9.5–28% [19] (pp. 615–628). However, most previous studies employed field-based correlative approaches under uncontrolled environmental conditions, making it difficult to isolate the specific effects of terminal heat stress from confounding factors such as soil moisture variability and nutrient availability. Moreover, these studies predominantly focused on yield components (grain number, thousand-grain weight) as endpoints, but failed to systematically quantify the relative contributions of photosynthetic capacity, assimilate partitioning, and sugar metabolism to grain-filling dynamics.

Terminal heat stress impairs grain filling by disrupting the post-anthesis source-flow-sink continuum. Flag leaves act as major source organs, supplying photosynthetically derived assimilates to developing grains [20] (pp. 268). High temperatures inhibit carbon assimilation both directly, through adverse effects on photosynthetic enzymes, and indirectly, through alterations in transpiration and stomatal conductance [21,22] (pp. 7351–7364, pp. 1452–1467). In particular, heat stress accelerates chlorophyll degradation and chloroplast senescence in flag leaves, thereby decreasing the photosynthetic rate [23–25] (pp. 1–11, pp. 476–490, pp. 1196–

1211). Because photochemical reactions and electron transport occur in thylakoid membranes, Photosystem II (PSII) is especially vulnerable to heat-induced disruption of electron carriers and membrane fluidity [26]. Consequently, heat stress impairs electron transport, reduces photochemical energy allocation and efficiency, and promotes excess excitation energy accumulation, ultimately suppressing carbon assimilation in wheat flag leaves [27–30] (pp. 616, pp. 1655–1660, pp. 185–192, pp. 2251). However, the quantitative links between chloroplast ultrastructural damage, PSII efficiency loss, sugar synthesis and export, and subsequent assimilate allocation to developing grains remain unclear, limiting the development of targeted heat-mitigation strategies.

Sugar, the primary product of photosynthesis, is essential for plant growth and has a major influence on plant quality and yield [31] (pp. 1–11). Heat-induced declines in photosynthetic capacity restrict carbon assimilation and consequently disturb sugar metabolism, the key link between source activity in flag leaves and sink demand in developing grains. Trehalose-6-phosphate (T6P), a low-abundance metabolite closely associated with sucrose status, coordinates carbon allocation and developmental transitions [32]. Recent evidence further suggests that endogenous trehalose and sucrose metabolism genes in wheat endosperm are transcriptionally regulated by developmental factors, directly influencing grain weight and filling efficiency [33]. Thus, heat-induced disruption of sucrose homeostasis may impair grain filling through T6P-mediated signaling. Sucrose synthesized in flag leaves is the major form of long-distance carbon transport and a direct precursor for starch synthesis in developing grains [34] (pp. 327–409). Trehalose, a non-reducing disaccharide, has been extensively documented as a stress protectant [35,36] (pp. 37–56, pp. 311–319). It acts both as an osmoprotectant that stabilizes membranes and as a signaling molecule regulating stress responses [37]. Trehalose metabolism is closely linked to T6P signaling: wheat TPP genes contribute to developmental regulation and stress adaptation [38], whereas T6P interacts with hormone-signaling pathways to modulate stress responses [39]. Under heat stress, exogenous trehalose reprograms transcriptomic and metabolic responses, enhancing heat-responsive genes, antioxidant metabolism, and stress signaling [40]. It also protects D1 protein integrity [41]. and promotes cyclic electron flow to maintain PSII function under heat and drought stress [42] (pp. 115–122). Moreover, trehalose may enhance photosynthetic carbon assimilation in a species-dependent manner and facilitate abiotic-stress memory [43] (pp. 770–776). These dynamic changes reflect disruptions in the source-sink-flow continuum that governs yield formation. However, previous research has treated photosynthesis (source), sugar metabolism (flow), and grain filling (sink) as isolated processes, failing to elucidate their coupling mechanisms under heat stress. Critically, the relative contributions of source capacity (photosynthetic rate), flow efficiency (sugar partitioning and transport), and sink strength (grain-filling rate) to final yield remain unquantified. Addressing this gap is essential for developing integrated mitigation approaches.

However, previous studies on exogenous trehalose in wheat under heat stress have predominantly focused on physiological responses at early developmental stages or single-organ systems. For example, it has been demonstrated that exogenous trehalose improves flag leaf physiological traits and yield under post-anthesis heat

stress through enhanced antioxidant capacity and photosynthetic performance [44] (pp. 2210–2224). However, such studies typically examined either source organs (e.g., flag leaves) or sink organs (e.g., grains) in isolation, without systematically investigating the coordinated source-sink-flow dynamics that underpin yield formation. Moreover, the underlying mechanisms linking trehalose-induced physiological changes to grain-filling processes-particularly the role of sugar metabolism in mediating source-sink communication-remain poorly understood.

Therefore, this study aimed to evaluate the effects of exogenous TRE on yield formation, photosynthetic characteristics, dry matter accumulation, and sugar metabolism in winter wheat under heat stress during grain filling, with the goal of providing a theoretical basis and practical guidance for mitigating terminal heat stress in wheat production.

2. Materials and Methods

2.1. Overview of the Experimental Field

The experiment was conducted from 2020 to 2022 at the High-Tech Park of Anhui Agricultural University, China (31.85°N, 117.27°E). The experimental site had brown soil, and its pre-sowing nutrient status is presented in **Table 1**. Maize was cultivated in the field during the preceding growing season.

Table 1. Nutrient content of the 0–20 cm soil layer in the experimental field before sowing.

Year	Total N ($g\ kg^{-1}$)	Organic Matter ($g\ kg^{-1}$)	Available Phosphorous ($mg\ kg^{-1}$)	Alkali Hydrolyzed Nitrogen ($mg\ kg^{-1}$)	Rapidly-Available Potassium ($mg\ kg^{-1}$)
2020–2021	0.89	14.21	21.51	77.15	238.11
2021–2022	1.03	13.07	18.25	64.41	203.51

2.2. Materials and Experimental Design

The field experiment was carried out over two consecutive wheat growing seasons (2020–2021 and 2021–2022). In the 2020–2021 season, seeds of eight candidate wheat genotypes were sown on October 30, 2020. Anthesis occurred on April 13, 2021, and plants were harvested at physiological maturity on May 25, 2021. In the 2021–2022 season, the two representative winter wheat cultivars, ‘Huaimai 33’ (HM33, heat-tolerant, originated in Huai’an, China) and ‘Fanmai 5’ (FM5, heat-sensitive, originated in Zhoukou, China), were sown on October 30, 2021, reached anthesis on April 11, 2022, and were harvested on May 22, 2022. The total growth duration for both cultivars across the two seasons was approximately 205–207 days. The two experimental wheat varieties, ‘Huaimai 33’ (HM33) and ‘Fanmai 5’ (FM5), were selected from eight candidate genotypes based on a preliminary field screening experiment conducted in 2020. To investigate the physiological responses of genotypes with contrasting heat tolerance, we evaluated the 1000-grain weight (TGW) and the Heat Susceptibility Index (HSI) of the eight candidates under post-anthesis heat stress. Among these genotypes, HM33 was identified as the most heat-tolerant

cultivar, exhibiting the lowest TGW reduction (9.09%) and HSI (0.74). Conversely, FM5 was identified as the most heat-sensitive cultivar, displaying the highest TGW reduction (14.01%) and HSI (1.14). Based on these contrasting traits, HM33 and FM5 were selected as the experimental materials. A split-plot design was employed, with varieties, TRE application (Dezhou Huiyang Biotechnology Co., Ltd., Dezhou, Shandong, China), and warming treatment assigned to the main plots, subplots, and split plots, respectively. A total of 5 treatments were set up: foliar spraying with clean water (the volume was the same as that of the TRE solution for spraying) + non-warming (CK); foliar spraying with clean water (the volume was the same as that of the TRE solution for spraying) + warming (H); foliar spraying with 10 mmol L^{-1} TRE + warming during grain filling ($T_{10}H$); foliar spraying with 15 mmol L^{-1} TRE + warming during grain filling ($T_{15}H$); and foliar spraying with 20 mmol L^{-1} TRE + warming during grain filling ($T_{20}H$). During anthesis, water and TRE solutions (99% purity) were applied once daily at dusk for three consecutive days. Each application was conducted at a rate of 100 mL m^{-2}, ensuring thorough wetting of both adaxial and abaxial leaf surfaces. Plants in the CK treatment were sprayed with the same volume of water used for the TRE treatments, as TRE was dissolved in water. Tween-20 was added to the TRE solution at 0.002 mL per 100 mL to facilitate the adsorption of exogenous substances on the leaf surface [24,45–47] (pp. 476–490, pp. 395–398, pp. 53, pp. 247–257). The area of each plot was 9 m^2 (3 m × 3 m). Each treatment was replicated 3 times. The treatments were randomly arranged. Furrowing and sowing were performed manually, with a target seedling density of 3.75 million plants ha^{-1}. During the growing season, nitrogen fertilizer was applied at 240 kg N ha^{-1} in three applications at a ratio of 5:3:2 (basal application: topdressing at the tillering stage: topdressing at the booting stage). Phosphorus and potassium fertilizers were applied entirely as basal fertilizers at rates of 100 kg P_2O_5 ha^{-1} and 150 kg K_2O ha^{-1}, respectively. All other cultivation and field-management practices followed those used for local high-yield wheat production.

A passive warming method was used to simulate the high-temperature environment during the daytime. Warming treatment was initiated 15 days after anthesis (DAA) and lasted for 5 consecutive days, with daily warming applied from 09:00 to 17:00 h. To monitor the microclimate, canopy air temperature and relative humidity inside and outside the warming sheds were continuously recorded at 10-min intervals. The average temperatures (**Figures 1A,B**) and representative diurnal temperature dynamic profiles (**Figures 1C,D**) inside and outside the sheds during the warming period (2020−2022) are shown in **Figure 1**. The mean increase in canopy air temperature during the grain-filling stage under high-temperature stress was 5.13 ℃.

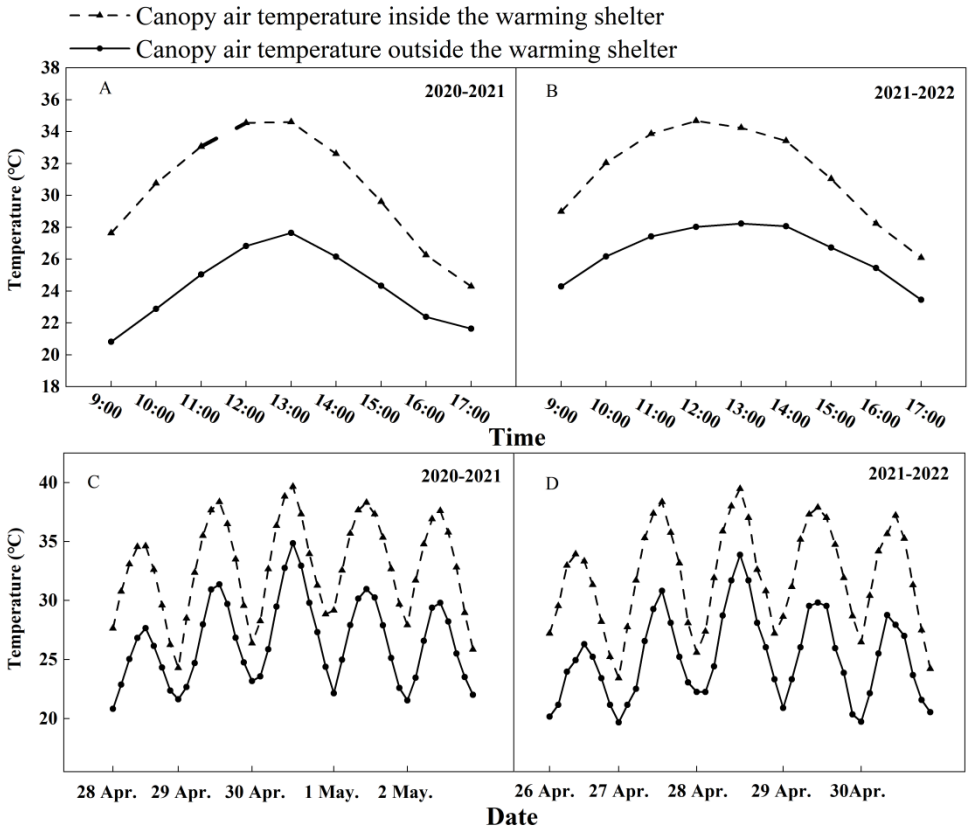

Figure 1. Average temperature (**A,B**) and dynamic diagram (**C,D**) of temperature changes inside and outside the shed during the test (2020–2022). A and C represent data from the 2020–2021, while B and D represent the 2021–2022.

2.3. Methods of Determination

2.3.1. Determination of Grain Yield

At physiological maturity, all wheat plants within a designated 0.5m area in each plot were harvested to determine the effective spike number. After threshing and air-drying, the grains were weighed and their moisture content was measured to calculate the actual grain yield adjusted to a standard 12.5% moisture content. For each plot, a representative air-dried grain sample of over 1000 g was collected for bulk density (test weight) determination, from which two subsamples of 1000 grains were randomly selected and weighed to obtain the mean thousand-kernel weight (TKW). In addition, 20 spikes were randomly selected per plot to measure spike length and count the number of grains per spike. The theoretical yield was calculated based on the effective spike number, grain number per spike, and thousand-kernel weight [48] (pp. 1–15).

At maturity, thirty wheat ears were randomly harvested from each treatment to assess grain filling characteristics. To investigate the spatial variations across different micro-positions on the spike, a two-dimensional classification was applied. First, vertically, each ear was systematically divided into three equal sections (namely, upper/apical, central, and lower/basal spikelets) along the rachis. Second, horizontally within an individual spikelet from any of these sections, individual grains were categorized based on their floret positions. Specifically, superior grains were defined as the basal one or two grains (first and second florets) of each spikelet, whereas

inferior grains comprised all remaining grains (third and subsequent florets) within the corresponding spikelet. This classification yielded six sub-categories (e.g., central-superior and central-inferior grains) for subsequent grain-weight analysis (**Table 2**).

Table 2. Effects of exogenous trehalose on the yield of wheat plants under heat stress during grain filling (2020–2022).

Time	Cultivar	Treatment	Spikes (10^4 hm^{-2})	Kernel Numbers Per Spikes	1000-Grains Weight (g)	Grain Yield (kg hm^{-2})
2020–2021	HM33	CK	603.33 ± 6.67^{a}	41.67 ± 0.88^{a}	48.69 ± 0.08^{a}	8899.35 ± 28.62^{a}
		H	596.67 ± 3.33^{a}	39.67 ± 1.76^{a}	44.26 ± 0.07^{e}	7939.33 ± 43.78^{e}
		$T_{10}H$	600.00 ± 11.55^{a}	40.00 ± 1.00^{a}	45.18 ± 0.05^{d}	8136.82 ± 20.67^{d}
		$T_{15}H$	593.33 ± 3.33^{a}	40.67 ± 0.67^{a}	46.84 ± 0.07^{b}	8498.10 ± 31.79^{b}
		$T_{20}H$	603.33 ± 12.02^{a}	40.33 ± 1.33^{a}	45.65 ± 0.03^{c}	8240.58 ± 33.91^{c}
	FM5	CK	610.00 ± 15.28^{a}	33.67 ± 0.33^{a}	50.35 ± 0.02^{a}	8792.43 ± 24.81^{a}
		H	630.00 ± 5.77^{a}	32.67 ± 0.33^{a}	43.29 ± 0.10^{e}	7560.66 ± 33.99^{e}
		$T_{10}H$	623.33 ± 18.56^{a}	33.00 ± 0.58^{a}	45.55 ± 0.04^{d}	7954.45 ± 24.80^{d}
		$T_{15}H$	623.33 ± 16.67^{a}	33.33 ± 0.33^{a}	47.52 ± 0.01^{b}	8298.44 ± 28.98^{b}
		$T_{20}H$	620.00 ± 10.00^{a}	33.33 ± 0.67^{a}	46.18 ± 0.03^{c}	8064.43 ± 33.58^{c}
	F-value	F-Cultivar	9.32**	150.82**	154.86**	307.89**
		F-Treatment	0.12	0.73	2813.16**	957.60**
		F-C×T	0.44	0.11	134.59**	14.51**
2021–2022	FM5	CK	610.00 ± 15.28^{a}	33.67 ± 0.33^{a}	49.24 ± 0.24^{a}	8581.49 ± 71.06^{a}
		H	630.00 ± 5.77^{a}	32.67 ± 0.33^{a}	43.29 ± 0.10^{d}	7544.60 ± 31.29^{d}
		$T_{10}H$	623.33 ± 18.56^{a}	33.00 ± 0.58^{a}	44.87 ± 0.37^{c}	7819.94 ± 112.52^{c}
		$T_{15}H$	623.33 ± 16.67^{a}	33.33 ± 0.33^{a}	46.08 ± 0.23^{b}	8029.47 ± 69.44^{b}
		$T_{20}H$	620.00 ± 10.00^{a}	33.33 ± 0.67^{a}	44.34 ± 0.04^{c}	7726.71 ± 33.85^{c}
	HM33	CK	603.33 ± 6.67^{a}	38.33 ± 1.33^{a}	48.74 ± 0.22^{a}	8655.83 ± 72.63^{a}
		H	596.67 ± 3.33^{a}	37.67 ± 0.67^{a}	41.90 ± 0.22^{d}	7833.72 ± 44.92^{d}
		$T_{10}H$	600.00 ± 11.55^{a}	38.33 ± 0.67^{a}	43.91 ± 0.21^{c}	8041.02 ± 34.35^{c}
		$T_{15}H$	593.33 ± 3.33^{a}	37.00 ± 0.00^{a}	47.61 ± 0.25^{b}	8257.04 ± 81.47^{b}

	$T_{20}H$	603.33 ± 12.02[a]	38.67 ± 0.88[a]	43.20 ± 0.41[c]	8021.22 ± 43.82[c]
	F-$_{Cultivar}$	2.81	187.57**	28.76	285.26**
F-$_{value}$	F-$_{Treatment}$	0.11	0.81	318.05**	64.25**
	F-$_{C×T}$	0.44	1.33	7.88**	3.64*

Note: CK: spray an equal amount of clean water on the leaf surface + no high temperature; H: spray an equal amount of clean water + high temperature; $T_{10}H$: spray 10 mmol L^{-1} trehalose + high temperature stress during filling; $T_{15}H$: spray 15 mmol L^{-1} trehalose + high temperature stress during filling; $T_{20}H$: spray 20 mmol L^{-1} trehalose + high temperature stress during filling. F-$_{Cultivar}$ represents the F value of the variety, and F-$_{Treatment}$ represents the F value of the treatment; F-$_{C×T}$ represents the F value of interaction between the breed and the treatment. Different lowercase letters indicate significant differences among treatments at $P < 0.05$. * Indicates reaching a significant level ($P < 0.05$), and ** indicates a very significant level ($P < 0.01$). Significant levels among different treatments in the same period were indicated by distinct lowercase letters ($P < 0.05$). HM33: Huaimai 33; FM5: Fanmai 5.

2.3.2. Determination of Dry Matter-Related Items

At both flowering and maturity stages, 30 representative single culms per plot were randomly sampled (avoiding the designated yield-determination areas) and separated into stems-leaves and spikes (no separation was performed at the jointing stage). The samples were heat-killed at 105 °C for 30 min, and then dried at 75 °C to a constant weight to determine the dry matter weight per culm. Based on the population dry matter accumulation at heading and maturity, the pre- and post-anthesis dry matter accumulation and translocation indices were calculated. Specifically, pre-anthesis measurements included dry matter accumulation, translocation amount, translocation efficiency, and its contribution rate to grain yield. Post-anthesis measurements included dry matter accumulation and its contribution rate to grain yield. The population dry matter accumulation was converted from the single-culm dry weight and the tiller density (number of stems and tillers per unit area) at the corresponding growth stages [42] (pp. 1–15).

2.3.3. Determination of the Net Photosynthetic Rate (P_n)

The net photosynthetic rate of flag leaves was determined at 21 and 28 days after anthesis (DAA). To ensure data reliability and minimize spatial variance, 12 representative flag leaves per treatment, characterized by uniform developmental stages and consistent light-receiving orientations within the canopy, were randomly selected for in vivo measurements. A LI-6400 portable photosynthesis system (LI-COR Biosciences, Lincoln, NE, USA) was used to determine the P_n. To avoid the midday depression of photosynthesis, all measurements were strictly conducted between 09:00 and 11:00 on clear, cloudless days. A leaf chamber equipped with a red/blue LED light source was used. All measurements were recorded at a constant flow rate of 500 mL min^{-1} and CO_2 concentration of ca. 380 μmol mol^{-1}, under a photosynthetically active radiation of 1000 μmol m^{-2} s^{-1} and relative humidity of 60%.

2.3.4. Determination of Chlorophyll Fluorescence-Related Parameters

The maximum photochemical efficiency of photosystem II (F_v/F_m) was measured on the same flag leaf using a PAM-2500 chlorophyll fluorometer (Heinz Walz GmbH, Effeltrich, Germany). The minimum and maximum chlorophyll fluorescence values (F_o and F_m, respectively) were determined, and F_v/F_m was calculated as follows: $F_v/F_m = (F_m - F_o)/F_m$ [49] (pp. 87–92).

2.3.5. Transmission Electron Microscopy Observation of Chloroplasts

Central segments of flag leaves were excised and cut into 1 mm² pieces with a razor blade. Samples were pre-fixed in glutaraldehyde fixative for 4 h, rinsed three times with phosphate buffer, then post-fixed in 1% osmium tetroxide (OsO_4, prepared with the same phosphate buffer) for 2–3 h, followed by identical buffer rinsing. Fixed specimens were dehydrated in a graded acetone series for 15 min per step. Infiltration was performed sequentially with mixtures of Epon 812 resin and acetone at volume ratios of 1:3, 1:1, and 3:1. Samples were embedded in 100% Epon 812 resin for 5 h at 30 °C, followed by polymerization at 60 °C for 36–48 h. Ultrathin sections were cut using an LKB V ultramicrotome (LKB, Bromma, Sweden), stained with uranyl acetate and lead citrate, and observed and photographed under a JEM-100CX Ⅱ transmission electron microscope (TEM JEOL Ltd., Tokyo, Japan).

2.3.6. Determination of Soluble Sugar, Sucrose, and Starch Contents

Soluble sugar content was determined by the anthrone colorimetric method [50] (pp. 772–777). A 0.1 g pulverized sample was suspended in 8 mL of distilled water and extracted in a boiling water bath for 20 min. After cooling, the homogenate was filtered, and the residue was washed repeatedly with distilled water to a final filtrate volume of 10 mL. A 0.2 mL aliquot was then diluted with 0.8 mL of distilled water, mixed with 5 mL of anthrone reagent, and incubated in a boiling water bath for 10 min. Upon rapid cooling, absorbance was measured at 620 nm against a reagent blank.

The sucrose content was determined using a resorcinol test [51] (pp. 60–70). A 0.1 g homogenized sample was extracted in distilled water in a boiling water bath for 30 min. The mixture was cooled, filtered, and the residue was re-extracted for 10 min. Both filtrates were pooled and adjusted to a final volume of 100 mL. A 0.5 mL aliquot of this extract was diluted with 1.5 mL of distilled water, followed by the sequential addition of phenol and concentrated sulfuric acid for color development. Absorbance was then recorded based on the standard curve protocol.

Starch content was determined using the anthrone colorimetric method [52] (pp. 34–36). The insoluble residue from the soluble sugar extraction was suspended in 20 mL of distilled water and gelatinized in a boiling water bath for 30 min. For hydrolysis, 9.2 mol L^{-1} perchloric acid was added, and the extraction continued for 15 min. After centrifugation, the remaining residue was repeatedly re-extracted with 10 mL of distilled water until the iodine test confirmed complete hydrolysis (absence of blue coloration). All supernatants were pooled and diluted to 100 mL. An aliquot was subsequently processed for starch quantification using the standard curve.

2.3.7. Starch Granule Morphology

Well-filled grains were selected and notched at the middle with a single-edged blade, perpendicular to the longitudinal axis. The grains were then held at both ends with forceps and gently fractured along the notch. Subsequently, a transverse section was made parallel to the fracture surface at approximately 2 mm from the initial cross-section. Sections with an intact central endosperm transverse surface were selected for observation and imaging using a scanning electron microscope (Philips XL-30 ESEM, Philips, Amsterdam, the Netherlands).

2.4. Statistical Analysis

All data are expressed as the mean ± standard deviation (SD) of three independent replicates. Differences among treatment groups within each experimental year were assessed using one-way analysis of variance (ANOVA), followed by Duncan's multiple range test. Statistical significance was defined at $P < 0.05$. Redundancy analysis (RDA) was conducted to evaluate relationships between environmental variables and response variables, while partial least squares regression (PLSR) was used to identify the major variables contributing to the observed responses. All statistical analyses were performed using SPSS Statistics (version 26.0; IBM Corp., Armonk, NY, USA), OriginPro 2026 (OriginLab Corp., Northampton, MA, USA), and Canoco 5 (Biometris, Wageningen, the Netherlands).

3. Results

3.1. Effect of Exogenous TRE on Wheat Yield and Its Components under Heat Stress

As shown in **Table 2**, heat stress (treatment H) significantly reduced grain yield in both wheat cultivars compared with the control (CK). Among the eight candidate genotypes, the heat-tolerant cultivar 'Huaimai 33' (HM33) exhibited the lowest yield reduction (9.09%), whereas the heat-sensitive cultivar 'Fanmai 5' (FM5) showed the greatest yield reduction (14.01%). This response was consistent with the contrasting heat tolerance of the two cultivars reported by previous studies [44] (pp. 2210–2224). Compared with the H treatment, foliar application of TRE increased grain yield in both cultivars. Application of 10, 15, and 20 mmol L^{-1} TRE increased grain yield by 2.28%, 5.47%, and 2.70%, respectively, in HM33, and by 4.43%, 8.09%, and 4.54%, respectively, in FM5. The greatest increase in grain yield was observed under the 15 mmol L^{-1} TRE treatment in both cultivars. The variation in thousand-grain weight was generally consistent with that in grain yield. Relative to the H treatment, thousand-grain weight increased by 2.28%, 5.46%, and 2.70% in HM33 and by 4.43%, 8.00%, and 4.53% in FM5 following the application of 10, 15, and 20 mmol L^{-1} TRE, respectively. In contrast, spike number and grain number per spike were not significantly affected by TRE application in either cultivar. Thus, the increase in grain yield following TRE application was primarily associated with the increase in thousand-grain weight. This result agrees with previous findings [44] (pp. 2210–2224). Notably, the TRE-induced improvement in grain yield was mainly associated with the maintenance of grain filling rather than with changes in sink number. Spike number and grain number per spike showed limited responses to TRE application, whereas thousand-grain weight and grain yield responded more clearly. These results indicate that the primary yield-related effect of exogenous TRE under terminal heat stress was the alleviation of heat-induced impairment of grain filling and grain weight formation.

3.2. Effect of Exogenous TRE on the Weight of Superior and Inferior Grains at Different Spike Positions under Heat Stress

The data in **Table 3** show that heat stress treatment significantly decreased the grain weight of both superior and inferior grain of heat-sensitive variety FM5

compared to the CK group, compared with the CK group (the same reference applies throughout this section unless otherwise stated). At the central spikelet position, the weights of superior and inferior grains decreased by 5.96% and 24.30%, respectively, under heat stress. Across all spikelet positions (upper, central, and lower), superior grains generally exhibited smaller weight reductions compared to inferior grains. For spikelets at the lower position of the spike, the weights of superior and inferior grains decreased by 29.70% and 7.45%, respectively. Overall, under heat stress, superior grains of the heat-tolerant variety HM33 exhibited slightly larger weight reduction percentages than inferior grains within each corresponding spikelet position. However, across the vertical spikelet positions, the grain weight reduction followed the order of upper > lower > middle for both grain types. The overall reduction in the grain weight was greater in FM5 than in HM33. In both FM5 and HM33, the greatest difference in grain weight reduction occurred between superior grains located at the upper and lower positions of the spike, reaching 54.97% and 68.77%, respectively. Under the 10, 15, and 20 mmol L^{-1} TRE treatments, the weight of superior grains at both the upper and lower spike positions in FM5 was significantly higher than that under treatment H. The greatest increase was observed in superior grains at the lower spike position, with increases of 8.44%, 13.34%, and 6.14%, respectively. Compared to treatment H, 10, 15, and 20 mmol L^{-1} TRE applications increased the weight of both superior and inferior grain in all positions on the spikes of HM33, and this increase for inferior grain was significantly higher than that for superior grain, with inferior grain in the lower positions showing the greatest increase (9.48, 9.80, and 2.91%, respectively). After TRE application, the increase in the weight of both superior and inferior grain in all positions on the spikes of FM5 was higher than that of HM33.

Table 3. Effects of exogenous trehalose on the weight of superior and inferior grains at the upper, central, and lower spikelet positions of wheat under heat stress during grain filling.

Cultivar	Treatment	Upper Spikelet		Central Spikelet		Lower Spikelet	
		Superior	Inferior	Superior	Inferior	Superior	Inferior
FM5	CK	50.31 ± 0.10^{a}	41.07 ± 0.21^{a}	53.38 ± 0.67^{a}	47.00 ± 0.47^{a}	55.59 ± 0.88^{a}	36.76 ± 0.75^{b}
	H	37.55 ± 0.16^{d}	30.33 ± 0.19^{d}	50.20 ± 0.88^{b}	35.58 ± 0.69^{c}	39.08 ± 0.09^{d}	34.02 ± 0.38^{c}
	$T_{10}H$	40.71 ± 0.54^{c}	32.50 ± 0.06^{b}	46.10 ± 0.34^{c}	36.36 ± 0.11^{c}	46.77 ± 0.77^{c}	31.17 ± 0.10^{d}
	$T_{15}H$	43.33 ± 0.31^{b}	31.43 ± 0.33^{c}	48.81 ± 0.29^{b}	36.19 ± 0.38^{c}	46.95 ± 0.70^{c}	35.61 ± 0.50^{b}
	$T_{20}H$	40.21 ± 0.06^{c}	26.11 ± 0.17^{e}	50.07 ± 0.92^{b}	39.13 ± 0.07^{b}	51.04 ± 0.37^{b}	42.10 ± 0.39^{a}
HM33	CK	44.48 ± 0.41^{a}	34.73 ± 0.28^{a}	56.55 ± 0.40^{a}	42.49 ± 0.20^{a}	54.25 ± 1.19^{a}	38.83 ± 0.59^{a}
	H	39.40 ± 0.36^{c}	32.60 ± 0.41^{b}	48.91 ± 0.26^{c}	37.24 ± 0.53^{b}	48.47 ± 0.78^{b}	35.33 ± 0.26^{a}
	$T_{10}H$	41.76 ± 0.61^{b}	33.98 ± 0.42^{ab}	51.20 ± 0.23^{b}	43.06 ± 0.30^{a}	48.65 ± 0.37^{b}	38.68 ± 2.90^{a}
	$T_{15}H$	38.57 ± 0.17^{c}	34.88 ± 0.51^{a}	49.05 ± 0.12^{c}	37.35 ± 0.27^{b}	49.28 ± 0.62^{b}	39.17 ± 0.63^{a}
	$T_{20}H$	39.87 ± 0.03^{c}	34.27 ± 0.53^{a}	46.17 ± 0.80^{d}	36.10 ± 0.80^{b}	47.00 ± 0.36^{b}	36.47 ± 1.39^{a}

	F-$_{\text{Cultivar}}$	18.96**	320.71**	13.16**	102.29**	143.27**	10.72**
F-$_{\text{value}}$	F-$_{\text{Treatment}}$	21.98**	27.36**	27.62**	23.18**	19.12**	5.75**
	F-$_{\text{C×T}}$	74.82**	27.80**	29.11**	49.84**	64.86**	9.91**

Note: CK: spray an equal amount of clean water on the leaf surface + no high temperature; H: spray an equal amount of clean water + high temperature; $T_{10}H$: spray 10 mmol L^{-1} trehalose + high temperature stress during filling; $T_{15}H$: spray 15 mmol L^{-1} trehalose + high temperature stress during filling; $T_{20}H$: spray 20 mmol L^{-1} trehalose + high temperature stress during filling. F-$_{\text{Cultivar}}$ represents the F value of the variety, and F-$_{\text{Treatment}}$ represents the F value of the treatment; F-$_{\text{C×T}}$ represents the F value of interaction between the breed and the treatment. * Indicates reaching a significant level ($P < 0.05$), and ** indicates a very significant level ($P < 0.01$). Significant levels among different treatments in the same period were indicated by distinct lowercase letters ($P < 0.05$). HM33: Huaimai 33; FM5: Fanmai 5.

3.3. Effect of Exogenous TRE on Dry Matter Accumulation and Allocation of Wheat under Heat Stress

Dry matter accumulation at 21 DAA was higher in the heat-tolerant cultivar HM33 than in the heat-sensitive cultivar FM5 in both 2021 and 2022 (**Figure 2A**). Heat stress during grain filling reduced dry matter accumulation in both cultivars, with greater reductions in total dry matter and organ dry matter observed in FM5 than in HM33. The total dry matter accumulation and dry matter accumulation in individual organs of FM5 were 37.09% lower than those of HM33. TRE application alleviated the heat-induced reduction in dry matter accumulation. Relative to the H treatment, $T_{10}H$, $T_{15}H$, and $T_{20}H$ increased leaf dry matter accumulation in HM33 by 0.89%, 2.19%, and 1.74%, respectively, and in FM5 by 12.39%, 14.89%, and 10.85%, respectively. In HM33, $T_{15}H$ increased dry matter accumulation in the upper three leaves relative to the H treatment, with a significant increase observed in the flag leaf.

At maturity, total dry matter accumulation remained higher in HM33 than in FM5 (**Figure 2B**). Heat stress significantly reduced total dry matter accumulation and dry matter accumulation in individual organs in both cultivars, and the reductions were more pronounced in FM5. Spike dry matter showed the greatest reduction, being 59.0% lower in FM5 than in HM33. Across the two growing seasons, heat stress caused a greater reduction in dry matter accumulation in the upper three leaves of FM5 than in HM33, particularly in the second leaf from the top. TRE application mitigated these reductions. Compared with the H treatment, $T_{10}H$, $T_{15}H$, and $T_{20}H$ increased dry matter accumulation in the upper three leaves by 2.01%, 11.35%, and 1.93%, respectively, in HM33, and by 7.43%, 20.34%, and 2.44%, respectively, in FM5. The effects of TRE on dry matter accumulation followed the order $T_{15}H > T_{10}H > T_{20}H$. Under $T_{15}H$, the increase in dry matter accumulation was 38.06% greater in FM5 than in HM33. However, the increase in flag-leaf dry matter did not differ significantly between the two cultivars.

At maturity, the H treatment significantly increased both the amount and proportion of dry matter allocated to stems, leaf sheaths, and leaves in FM5 and HM33 relative to the CK treatment, whereas both the amount and proportion of dry matter allocated to grains were significantly reduced (**Table 4**). Under TRE application, dry matter allocation to stems, leaf sheaths, and leaves followed the order $T_{20}H > T_{10}H > T_{15}H$ in both cultivars. In contrast, all TRE treatments increased the amount and proportion of dry matter allocated to grains relative to the H treatment. Compared with $T_{10}H$ and $T_{20}H$, $T_{15}H$ increased the proportion of dry matter allocated to grains by 2.28%

and 4.89%, respectively, in FM5 and by 2.78% and 4.56%, respectively, in HM33. Overall, TRE increased dry matter accumulation per plant and dry matter allocation to grains while reducing the proportion of dry matter retained in vegetative organs. The enhancement of post-anthesis dry matter accumulation and grain dry matter allocation under TRE treatment was consistent with the increases in thousand-grain weight and grain yield. These results suggest that TRE may alleviate heat-induced impairment of grain filling by promoting the utilization and redistribution of post-anthesis assimilates toward developing grains.

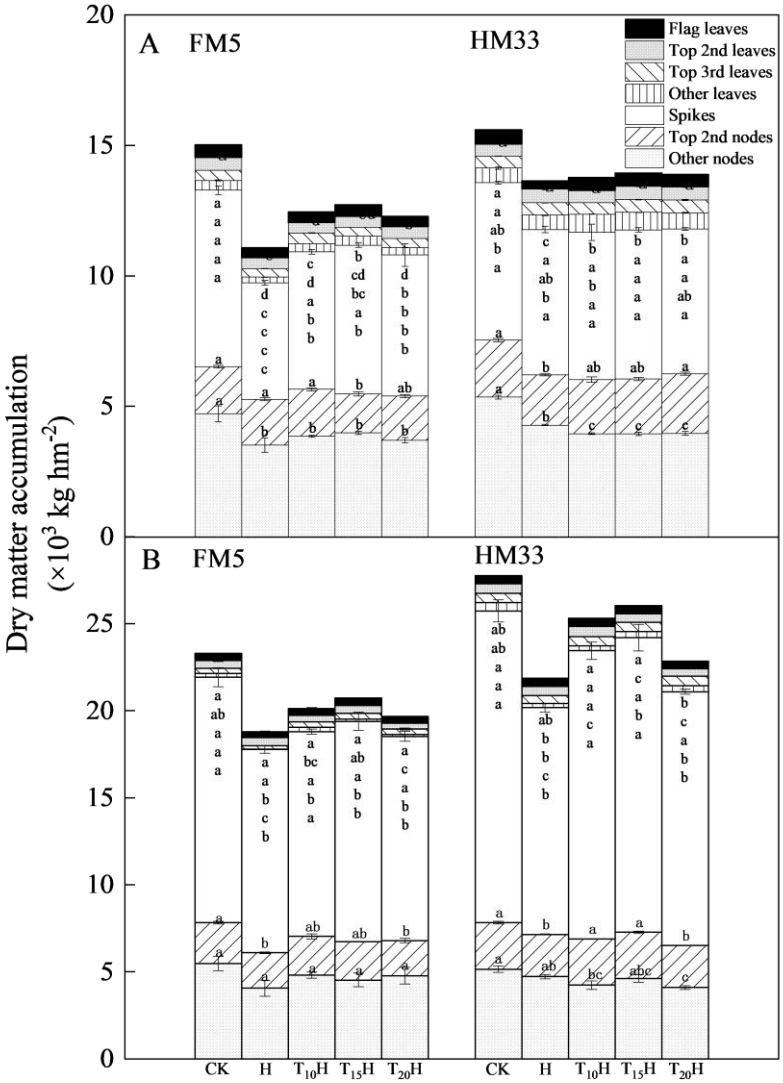

Figure 2. Effects of exogenous trehalose on dry matter accumulation in FM5 and HM33 under heat stress during grain filling at 21 d after flowering and at the maturity stage. Note: CK: spray an equal amount of clean water on the leaf surface + no high temperature; H: spray an equal amount of clean water + high temperature; $T_{10}H$: spray 10 mmol L^{-1} trehalose + high temperature stress during filling; $T_{15}H$: spray 15 mmol L^{-1} trehalose + high temperature stress during filling; $T_{20}H$: spray 20 mmol L^{-1} trehalose + high temperature stress during filling. Different lowercase letters represent significant levels among different treatments in the same period ($P < 0.05$). FM5: Fanmai 5; HM33: Huaimai 33; A: 21 DAA; B: Maturity stage.

Table 4. Effects of exogenous trehalose on the amount and proportion of dry matter allocation to different organs at the maturity stage of FM5 and HM33 plants under heat stress during grain filling.

Cultivar	Treatment	Stem+Sheath+Leaf		Spike-Stalk+Glume		Grain	
		Amount (kg hm^{-2})	Rate (%)	Amount (kg hm^{-2})	Rate (%)	Amount (kg hm^{-2})	Rate (%)
FM5	CK	5961.73 ± 32.57^{e}	34.66 ± 0.19^{d}	2315.55 ± 27.04^{e}	13.73 ± 0.13^{e}	8581.49 ± 71.06^{a}	50.90 ± 0.26^{a}
	H	6801.53 ± 27.08^{a}	40.35 ± 0.24^{a}	2853.86 ± 16.21^{a}	16.59 ± 0.07^{a}	7544.60 ± 31.29^{d}	43.86 ± 0.17^{e}
	$T_{10}H$	6248.23 ± 14.51^{c}	37.33 ± 0.08^{c}	2451.44 ± 24.22^{c}	14.84 ± 0.16^{c}	7819.94 ± 112.52^{c}	47.34 ± 0.30^{c}
	$T_{15}H$	6177.17 ± 9.36^{d}	37.39 ± 0.07^{c}	2376.69 ± 4.42^{d}	14.33 ± 0.03^{d}	8029.47 ± 69.44^{b}	48.42 ± 0.10^{b}
	$T_{20}H$	6471.80 ± 7.35^{b}	39.03 ± 0.14^{b}	2539.30 ± 13.06^{b}	15.17 ± 0.06^{b}	7726.71 ± 33.85^{c}	46.16 ± 0.10^{d}
HM33	CK	6624.89 ± 53.08^{d}	36.93 ± 0.16^{d}	2656.65 ± 26.07^{e}	14.81 ± 0.16^{e}	8655.83 ± 46.60^{a}	48.26 ± 0.23^{a}
	H	7440.42 ± 45.03^{a}	40.42 ± 0.20^{a}	3132.14 ± 22.20^{a}	17.02 ± 0.14^{a}	7833.72 ± 28.82^{d}	42.56 ± 0.16^{e}
	$T_{10}H$	6982.34 ± 36.24^{c}	39.10 ± 0.13^{b}	2832.95 ± 25.32^{c}	15.86 ± 0.12^{c}	8041.02 ± 22.04^{c}	45.03 ± 0.20^{c}
	$T_{15}H$	6868.27 ± 31.65^{c}	38.50 ± 0.17^{c}	2715.33 ± 15.34^{d}	15.22 ± 0.09^{d}	8257.04 ± 52.27^{b}	46.28 ± 0.26^{b}
	$T_{20}H$	7154.32 ± 47.92^{b}	39.48 ± 0.11^{b}	2946.66 ± 21.87^{b}	16.26 ± 0.09^{b}	8021.22 ± 28.11^{c}	44.26 ± 0.17^{d}
F-value	F-$_{Cultivar}$	9.47**	134.30**	171.71**	75.22**	441.91**	21.36**
	F-$_{Treatment}$	4.65**	9.07**	9.22**	18.85**	97.15**	47.01**
	F-$_{C\times T}$	5.01**	5.32**	6.98**	4.92**	7.22**	1.44

Note: CK: spray an equal amount of clean water on the leaf surface + no high temperature; H: spray equal amount of clean water + high temperature; $T_{10}H$: spray 10 mmol L^{-1} trehalose + high temperature stress during filling; $T_{15}H$: spray 15 mmol L^{-1} trehalose + high temperature stress during filling; $T_{20}H$: spray 20 mmol L^{-1} trehalose + high temperature stress during filling. F-$_{Cultivar}$ represents the F value of the variety, and F-$_{Treatment}$ represents the F value of the treatment; F-$_{C\times T}$ represents the F value of interaction between the breed and the treatment. * Indicates reaching a significant level ($P < 0.05$), and ** indicates a very significant level ($P < 0.01$). Significant levels among different treatments in the same period were indicated by distinct lowercase letters ($P < 0.05$). HM33: Huaimai 33; FM5: Fanmai 5.

3.4. Effect of Exogenous TRE on Net Photosynthetic Rate and Maximum Photochemical Efficiency of Flag Leaves under Heat Stress

Under heat stress during grain filling, the net photosynthetic rate (P_n) of the heat-tolerant cultivar HM33 and the heat-sensitive cultivar FM5 decreased by 20.19% and

27.40%, respectively, at 21 DAA, and by 55.27% and 61.54%, respectively, at 28 DAA, relative to the CK treatment (**Figure 3**). The heat-induced reduction in P_n was more pronounced at 28 DAA than at 21 DAA and was consistently greater in FM5 than in HM33. TRE application significantly increased P_n relative to the H treatment. At 21 DAA, $T_{10}H$, $T_{15}H$, and $T_{20}H$ increased P_n by 2.05%, 12.97%, and 1.44%, respectively, in HM33 and by 13.83%, 19.08%, and 11.69%, respectively, in FM5. At 28 DAA, P_n under $T_{15}H$ was significantly higher than that under $T_{10}H$ and $T_{20}H$, whereas no significant difference was observed between $T_{10}H$ and $T_{20}H$. Overall, the effectiveness of TRE treatments in alleviating heat-induced photosynthetic inhibition followed the order $T_{15}H > T_{10}H > T_{20}H$.

The maximum photochemical efficiency of PSII (F_v/F_m) was significantly higher at 21 DAA than at 28 DAA in both cultivars under all treatments (**Figure 3**). Heat stress significantly decreased F_v/F_m relative to the CK treatment. In HM33, F_v/F_m under the H treatment decreased by 9.06% and 14.94% at 21 and 28 DAA, respectively, whereas the corresponding reductions in FM5 were 10.58% and 20.03%. Thus, HM33 exhibited a smaller heat-induced reduction in F_v/F_m than FM5. TRE application alleviated the decline in F_v/F_m. Compared with the H treatment, $T_{10}H$, $T_{15}H$, and $T_{20}H$ increased F_v/F_m in HM33 by 3.97%, 4.55%, and 2.11%, respectively, at 21 DAA and by 3.22%, 6.25%, and 0.78%, respectively, at 28 DAA. The effectiveness of TRE treatments in mitigating the reduction in F_v/F_m followed the order $T_{15}H > T_{10}H > T_{20}H$. Compared with HM33, the mitigating effects of $T_{10}H$, $T_{15}H$, and $T_{20}H$ on the F_v/F_m reduction in FM5 were 2.97%, 4.56%, and 3.88% greater, respectively, at 21 DAA, and 3.13%, 5.89%, and 0.76% greater, respectively, at 28 DAA.

The maintenance of flag-leaf photosynthetic capacity under TRE treatment constituted the source basis for the subsequent improvement in dry matter accumulation, assimilate allocation, and grain filling. The alleviation of heat-induced declines in P_n and F_v/F_m indicates that TRE helped preserve carbon assimilation capacity and PSII photochemical activity during grain filling. This improved source activity was consistent with the subsequent changes in dry matter accumulation and grain-related traits, supporting a coordinated relationship between source maintenance and sink filling under terminal heat stress.

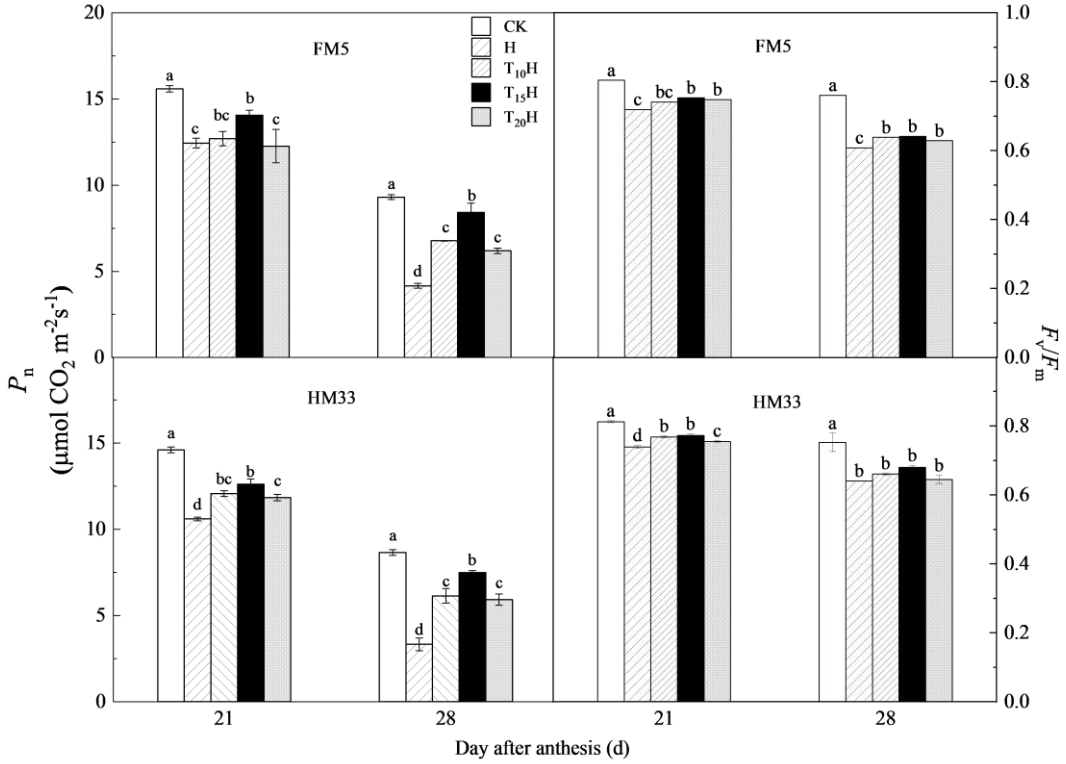

Figure 3. Effects of exogenous trehalose on the flag leaf net photosynthetic rate (P_n) and maximum photochemical efficiency (F_v/F_m) of FM5 and HM33 under heat stress during grain filling. Note: CK: spray an equal amount of clean water on the leaf surface + no high temperature; H: spray an equal amount of clean water + high temperature; $T_{10}H$: spray 10 mmol L^{-1} trehalose + high temperature stress during filling; $T_{15}H$: spray 15 mmol L^{-1} trehalose + high temperature stress during filling; $T_{20}H$: spray 20 mmol L^{-1} trehalose + high temperature stress during filling. Different lowercase letters represent significant levels among different treatments in the same period ($P < 0.05$). FM5: Fanmai 5; HM33: Huaimai 33.

3.5. Effect of Exogenous TRE on Chloroplast Ultrastructure of Flag Leaves under Heat Stress

Relative to the CK, heat stress during grain filling induced pronounced ultrastructural damage to chloroplasts (**Figure 4**). Chloroplasts became swollen, and partial disruption of the plasma membrane and chloroplast envelope was observed. The grana lamellae were deformed, curved, and discontinuous, accompanied by an increased number of osmiophilic granules. In contrast, under TRE treatments, chloroplasts were more closely appressed to the cell wall than those under the H treatment, while the plasma membrane and chloroplast envelope remained relatively intact. Only occasional discontinuities were observed in the grana lamellae, and the number of osmiophilic granules gradually decreased. Among the TRE treatments, $T_{15}H$ most effectively alleviated heat stress-induced chloroplast damage.

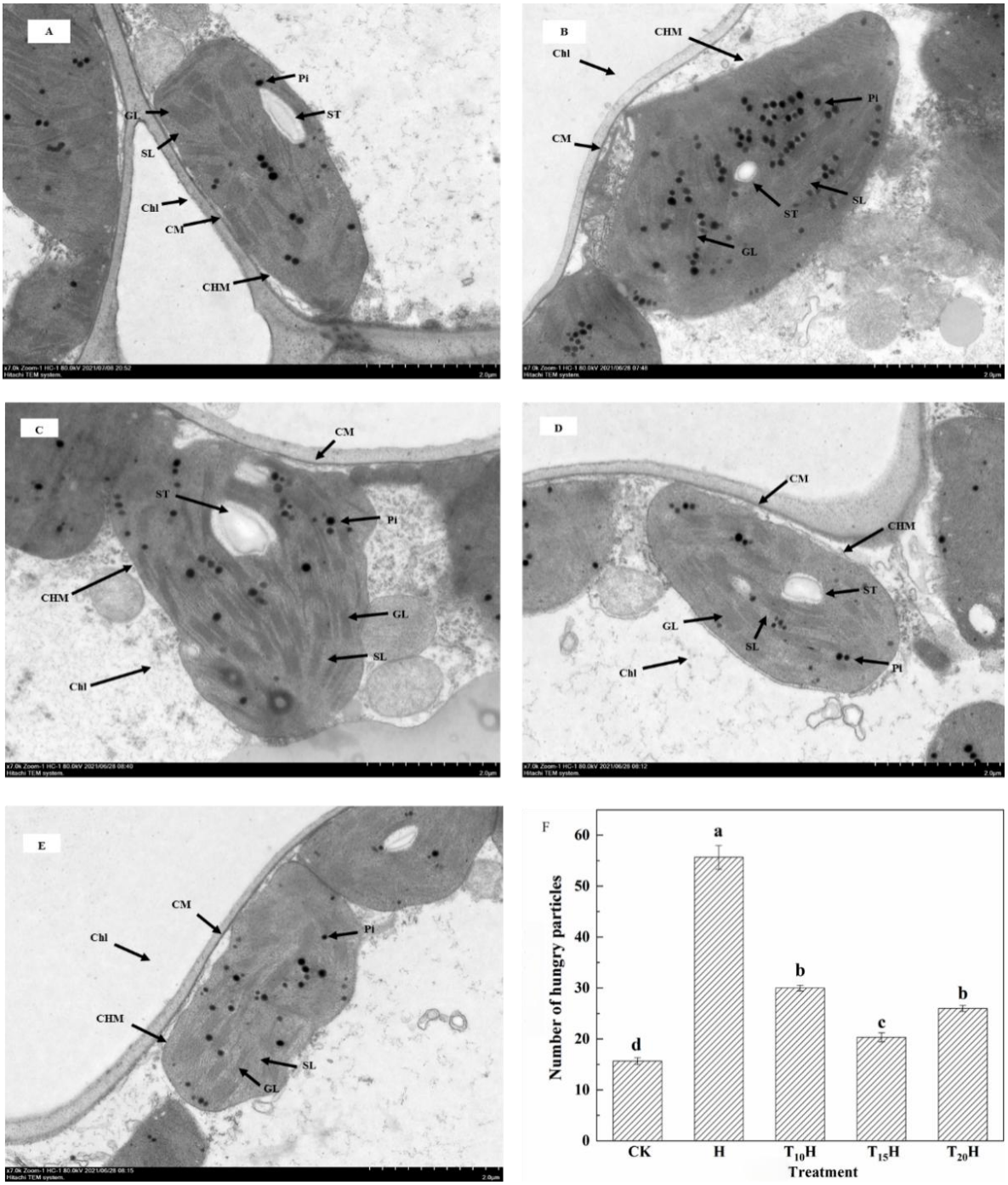

Figure 4. Effects of exogenous trehalose on the chloroplasts in the flag leaves of FM5 under heat stress during grain filling. Note: CK: spray an equal amount of clean water on the leaf surface + no high temperature; H: spray an equal amount of clean water + high temperature; $T_{10}H$: spray 10 mmol L^{-1} trehalose + high temperature stress during filling; $T_{15}H$: spray 15 mmol L^{-1} trehalose + high temperature stress during filling; $T_{20}H$: spray 20 mmol L^{-1} trehalose + high temperature stress during filling. Different lowercase letters represent significant levels among different treatments in the same period ($P < 0.05$). Chl: Chloroplast; CM: Cell membrane; CHM: Chloroplast membrane; GL: Substrate sheet layer; SL: Substrate layer; Pi: Osmiophilic granules; ST: Starch granules; A: CK processing; B: H treatment; C: $T_{10}H$ treatment; D: $T_{15}H$ treatment; E: $T_{20}H$ treatment; F: The number of Osmiophilic granules in chloroplasts. Scale bar = 2.0 μm

3.6. Effect of Exogenous TRE on the Contents of Trehalose, Soluble Sugar, Sucrose, and Starch in Flag Leaves under Heat Stress

TRE treatments in flag leaves were significantly lower at 28 DAA than at 21 DAA across all treatments in both cultivars (**Figure 5**). Heat stress during grain filling significantly increased endogenous TRE treatments relative to the CK. Compared with CK, TRE treatments in the heat-tolerant cultivar HM33 increased by 13.34% and 10.01% at 21 and 28 DAA, respectively, whereas the corresponding increases in the heat-sensitive cultivar FM5 were 16.55% and 11.59%. Thus, the heat-induced increase in TRE treatments was smaller in HM33 than in FM5. Exogenous TRE application further increased TRE treatments under heat stress. In HM33, compared with the H treatment, $T_{10}H$, $T_{15}H$, and $T_{20}H$ increased TRE treatments by 18.53%, 27.37%, and 8.74%, respectively, at 21 DAA and by 10.66%, 21.04%, and 5.12%, respectively, at 28 DAA. In FM5, the corresponding increases were 28.79%, 39.61%, and 18.11% at 21 DAA and 23.49%, 29.32%, and 14.55% at 28 DAA. The effects of the TRE treatments on increasing TRE treatments followed the order $T_{15}H > T_{10}H > T_{20}H$ in both cultivars. Moreover, the increase in TRE treatments induced by exogenous TRE was greater in FM5 than in HM33 and was more pronounced at 21 DAA than at 28 DAA. The changes in carbohydrate metabolism further support the connection between source activity, assimilate flow, and sink filling. The maintenance of soluble sugar, sucrose, and starch metabolism in flag leaves under TRE treatment indicates that carbon assimilation products remained metabolically available during grain filling. As sucrose is the main transport form of photoassimilates and starch serves as an important transient carbon reserve, the maintenance of carbohydrate metabolism may have facilitated the subsequent utilization and allocation of assimilates for grain filling. This interpretation is consistent with the improvement in grain weight and final grain yield observed under TRE treatment.

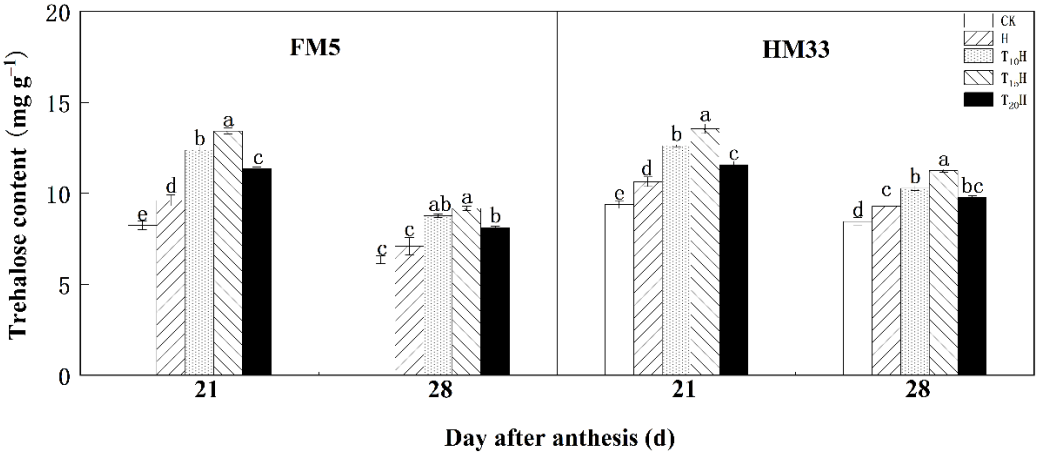

Figure 5. Effects of exogenous trehalose on trehalose content in flag leaves of Fanmai 5 and Huaimai 33 under high temperature stress during the grain filling period. Note: CK: spray an equal amount of clean water on the leaf surface + no high temperature; H: spray an equal amount of clean water + high temperature; $T_{10}H$: spray 10 mmol L^{-1} trehalose + high temperature stress during filling; $T_{15}H$: spray 15 mmol L^{-1} trehalose + high temperature stress during filling; $T_{20}H$: spray 20 mmol L^{-1} trehalose + high

temperature stress during filling. Different lowercase letters represent significant levels among different treatments in the same period ($P < 0.05$). FM5: Fanmai 5; HM33: Huaimai 33.

As shown in **Figure 6**, at 21 DAA, the soluble sugar content of both HM33 and FM5 was significantly higher under $T_{15}H$ than under $T_{10}H$ and $T_{20}H$. Across all TRE treatments, the soluble sugar content at 21 DAA was 9.33% and 34.27% higher than that at 28 DAA in HM33 and FM5, respectively. At both 21 and 28 DAA, the soluble sugar content of FM5 under $T_{10}H$, $T_{15}H$, and $T_{20}H$ was 9.02%, 11.63%, and 2.84% higher, respectively, than that of HM33. The effectiveness of the TRE treatments in alleviating the reduction in soluble sugar content followed the order: $T_{15}H > T_{10}H > T_{20}H$.

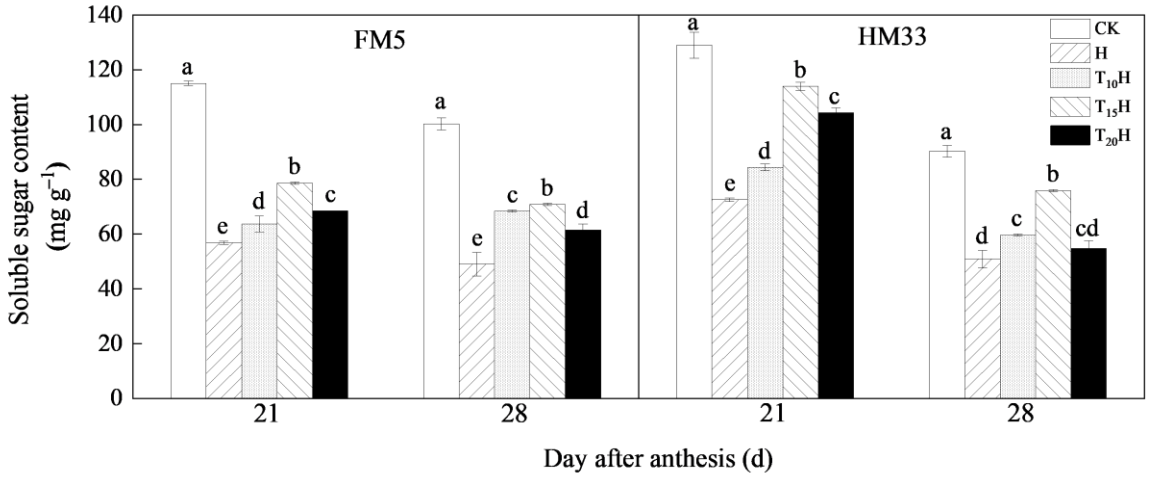

Figure 6. Effects of exogenous trehalose on the soluble sugar content of the flag leaf in FM5 and HM33 under heat stress during grain filling. Note: CK: spray an equal amount of clean water on the leaf surface + no high temperature; H: spray an equal amount of clean water + high temperature; $T_{10}H$: spray 10 mmol L^{-1} trehalose + high temperature stress during filling; $T_{15}H$: spray 15 mmol L^{-1} trehalose + high temperature stress during filling; $T_{20}H$: spray 20 mmol L^{-1} trehalose + high temperature stress during filling. Different lowercase letters represent significant levels among different treatments in the same period ($P < 0.05$). FM5: Fanmai 5; HM33: Huaimai 33.

As shown in **Figure 7**, sucrose content in flag leaves was significantly lower at 28 DAA than at 21 DAA. Under heat stress during grain filling, sucrose content decreased significantly relative to the CK. In the heat-tolerant cultivar HM33, sucrose content decreased by 26.72% and 22.62% at 21 and 28 DAA, respectively, whereas the corresponding decreases in the heat-sensitive cultivar FM5 were 33.68% and 30.14%. Exogenous TRE application alleviated the heat stress-induced reduction in sucrose content. Compared with the H treatment, sucrose content in HM33 under $T_{10}H$, $T_{15}H$, and $T_{20}H$ increased by 5.11%, 15.82%, and 8.56%, respectively, at 21 DAA, and by 3.57%, 9.15%, and 5.37%, respectively, at 28 DAA. Overall, the increase in sucrose content was greater at 28 DAA than at 21 DAA. In FM5, sucrose content under $T_{10}H$, $T_{15}H$, and $T_{20}H$ increased by 9.76%, 20.47%, and 8.29%, respectively, at 21 DAA, and by 8.39%, 7.11%, and 1.99%, respectively, at 28 DAA, compared with that in HM33.

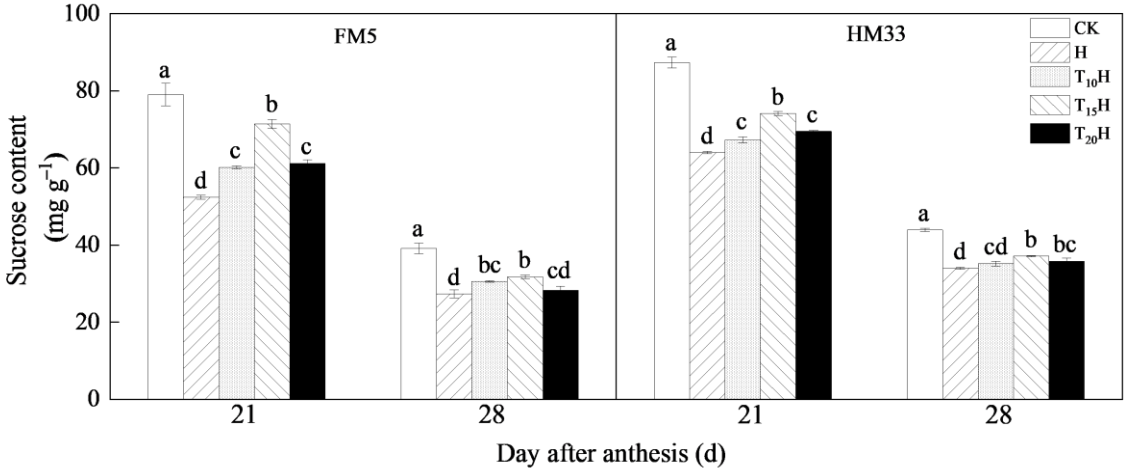

Figure 7. Effects of exogenous trehalose on the sucrose content of the flag leaf in FM5 and HM33 under heat stress during grain filling. Note: CK: spray an equal amount of clean water on the leaf surface + no high temperature; H: spray an equal amount of clean water + high temperature; $T_{10}H$: spray 10 mmol L^{-1} trehalose + high temperature stress during filling; $T_{15}H$: spray 15 mmol L^{-1} trehalose + high temperature stress during filling; $T_{20}H$: spray 20 mmol L^{-1} trehalose + high temperature stress during filling. Different lowercase letters represent significant levels among different treatments in the same period ($P < 0.05$). FM5: Fanmai 5; HM33: Huaimai 33.

3.7. Effect of Exogenous TRE on Soluble Sugar Content in Wheat Grains under Heat Stress

As shown in **Figure 8**, grain soluble sugar content was significantly lower at 28 DAA than at 21 DAA. Under heat stress during grain filling, grain soluble sugar content decreased significantly relative to the CK. In the heat-tolerant cultivar HM33, the reductions were 18.09% and 15.38% at 21 and 28 DAA, respectively, while the corresponding reductions in the heat-sensitive cultivar FM5 were 21.88% and 16.46%. Exogenous TRE application alleviated the heat stress-induced reduction in grain soluble sugar content. Compared with the H treatment, grain soluble sugar content in HM33 under $T_{10}H$, $T_{15}H$, and $T_{20}H$ increased by 8.17%, 11.25%, and 5.02%, respectively, at 21 DAA, and by 4.92%, 8.62%, and 3.79%, respectively, at 28 DAA. In FM5, grain soluble sugar content under $T_{10}H$, $T_{15}H$, and $T_{20}H$ increased by 3.84%, 4.27%, and 3.85%, respectively, at 21 DAA, and by 6.85%, 4.39%, and 3.28%, respectively, at 28 DAA, compared with that in HM33. Overall, the effectiveness of TRE treatments in mitigating the reduction in grain soluble sugar content followed the order: $T_{15}H > T_{10}H > T_{20}H$.

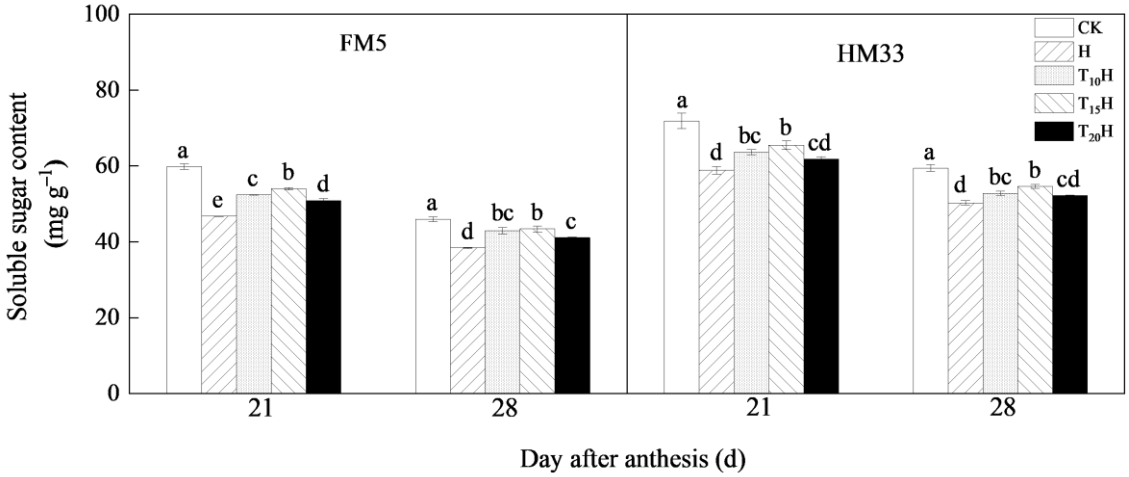

Figure 8. Effects of exogenous trehalose on the soluble sugar content of the grain in FM5 and HM33 under heat stress during grain filling. Note: CK: spray an equal amount of clean water on the leaf surface + no high temperature; H: spray an equal amount of clean water + high temperature; $T_{10}H$: spray 10 mmol L^{-1} trehalose + high temperature stress during filling; $T_{15}H$: spray 15 mmol L^{-1} trehalose + high temperature stress during filling; $T_{20}H$: spray 20 mmol L^{-1} trehalose + high temperature stress during filling. Different lowercase letters represent significant levels among different treatments in the same period ($P < 0.05$). FM5: Fanmai 5; HM33: Huaimai 33.

3.8. Effect of Exogenous TRE on Sucrose Content in Wheat Grains under Heat Stress

As shown in **Figure 9**, grain sucrose content in both HM33 and FM5 was significantly lower at 28 DAA than at 21 DAA under all treatments. Heat stress during grain filling (H treatment) significantly reduced grain sucrose content relative to the CK. Specifically, grain sucrose content in the heat-tolerant cultivar HM33 decreased by 19.98% and 18.93% at 21 and 28 DAA, respectively, whereas the corresponding reductions in the heat-sensitive cultivar FM5 were 24.72% and 23.10%. Thus, the heat stress-induced reduction in grain sucrose content was greater in FM5 than in HM33. Exogenous TRE application alleviated the heat stress-induced reduction in grain sucrose content. Compared with the H treatment, grain sucrose content in HM33 under $T_{10}H$, $T_{15}H$, and $T_{20}H$ increased by 9.16%, 15.89%, and 7.22%, respectively, at 21 DAA, and by 7.01%, 14.02%, and 3.64%, respectively, at 28 DAA. The effectiveness of the TRE treatments in mitigating the reduction in grain sucrose content followed the order: $T_{15}H > T_{20}H > T_{10}H$. Similarly, in FM5, grain sucrose content under $T_{10}H$, $T_{15}H$, and $T_{20}H$ increased by 15.94%, 20.66%, and 10.36%, respectively, at 21 DAA, and by 7.01%, 14.02%, and 3.64%, respectively, at 28 DAA, compared with the H treatment. The ranking of the TRE treatments in FM5 was consistent with that observed in HM33: $T_{15}H > T_{20}H > T_{10}H$.

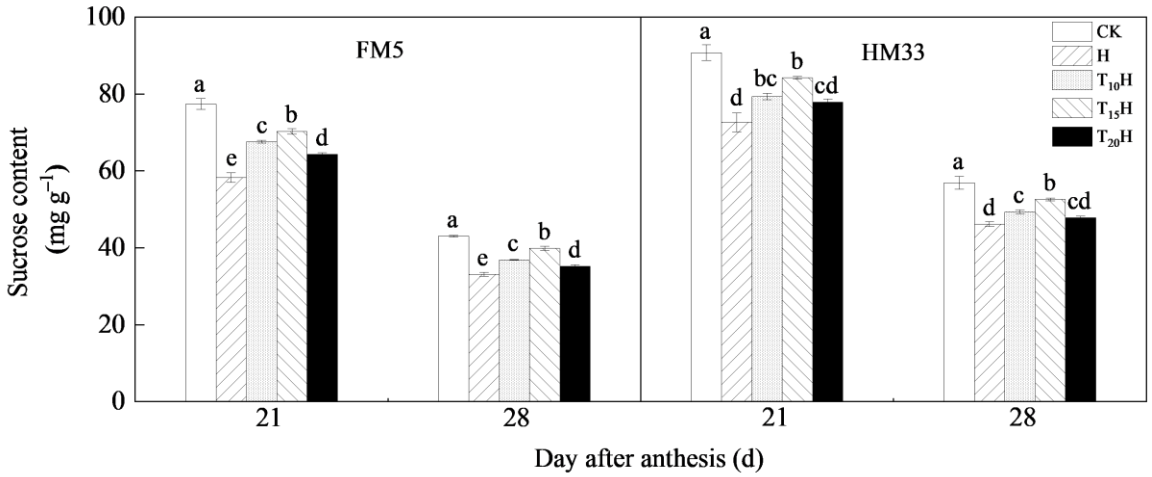

Figure 9. Effects of exogenous trehalose on the sucrose content of the grain in FM5 and HM33 under heat stress during grain filling. Note: CK: spray an equal amount of clean water on the leaf surface + no high temperature; H: spray an equal amount of clean water + high temperature; $T_{10}H$: spray 10 mmol L^{-1} trehalose + high temperature stress during filling; $T_{15}H$: spray 15 mmol L^{-1} trehalose + high temperature stress during filling; $T_{20}H$: spray 20 mmol L^{-1} trehalose + high temperature stress during filling. Different lowercase letters represent significant levels among different treatments in the same period ($P < 0.05$). FM5: Fanmai 5; HM33: Huaimai 33.

3.9. Effect of Exogenous TRE on Starch Content in Wheat Grains under Heat Stress

As shown in **Figure 10**, grain starch content was significantly higher at 28 DAA than at 21 DAA. Heat stress during grain filling significantly reduced grain starch content relative to the CK. In the heat-tolerant cultivar HM33, grain starch content decreased by 14.31% and 13.08% at 21 and 28 DAA, respectively. In the heat-sensitive cultivar FM5, the corresponding reductions were 23.74% and 18.43%. Overall, the heat stress-induced reduction in grain starch content was lower in HM33 than in FM5. Exogenous TRE application alleviated the reduction in grain starch content caused by heat stress. Compared with the H treatment, grain starch content in HM33 under $T_{10}H$, $T_{15}H$, and $T_{20}H$ increased by 5.72%, 9.02%, and 2.71%, respectively, at 21 DAA, and by 4.40%, 8.58%, and 1.59%, respectively, at 28 DAA. In FM5, grain starch content under $T_{10}H$, $T_{15}H$, and $T_{20}H$ increased by 12.62%, 14.66%, and 9.78%, respectively, at 21 DAA, and by 4.47%, 5.68%, and 4.99%, respectively, at 28 DAA, compared with that in HM33.

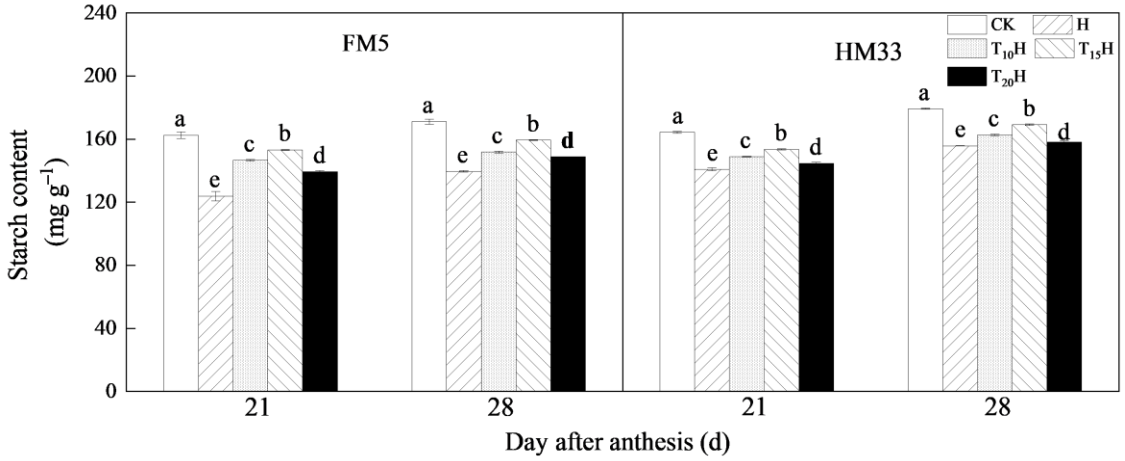

Figure 10. Effects of exogenous trehalose on the starch content of grain in FM5 and HM33 under heat stress during grain filling. Note: CK: spray an equal amount of clean water on the leaf surface + no high temperature; H: spray an equal amount of clean water + high temperature; $T_{10}H$: spray 10 mmol L^{-1} trehalose + high temperature stress during filling; $T_{15}H$: spray 15 mmol L^{-1} trehalose + high temperature stress during filling; $T_{20}H$: spray 20 mmol L^{-1} trehalose + high temperature stress during filling. Different lowercase letters represent significant levels among different treatments in the same period ($P < 0.05$). FM5: Fanmai 5; HM33: Huaimai 33.

3.10. Effect of Exogenous TRE on Starch Granule Morphology of Wheat Grains under Heat Stress

As shown in **Figure 11**, compared with the CK, heat stress induced varying degrees of deformation in wheat starch granules. Specifically, A-type starch granules exhibited reduced size, more pronounced surface indentations, and enlarged cracks and micropores. B-type starch granules changed from having smooth surfaces to irregular polygonal shapes, while C-type starch granules also became irregularly polygonal. Under TRE treatment, A-type starch granules were predominantly spherical or elliptical, with increased size and abundance, although micropores were observed on their surfaces. In contrast, B- and C-type starch granules exhibited only slight surface shrinkage.

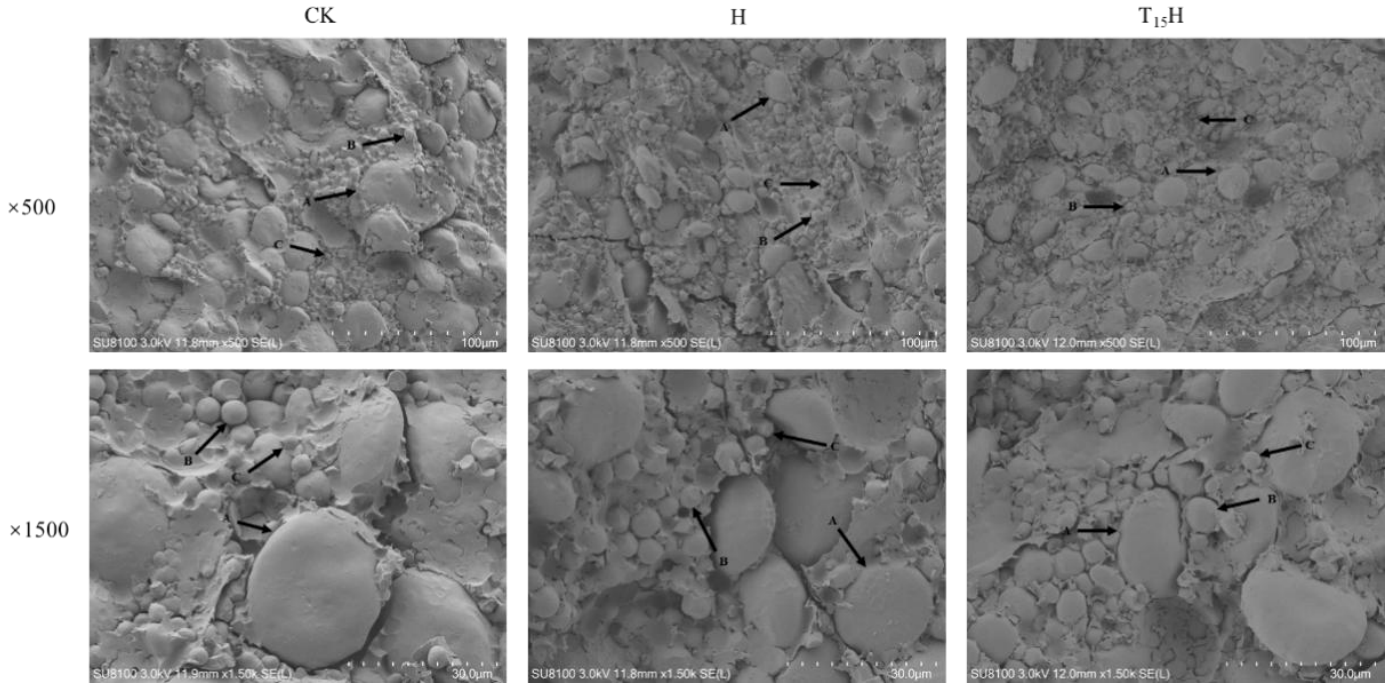

Figure 11. Effects of exogenous trehalose on starch granule morphology at the maturity stage in FM5 under heat stress during grain filling. Note: CK: spray an equal amount of clean water on the leaf surface + no high temperature; H: spray an equal amount of clean water + high temperature; $T_{15}H$: spray 15 mmol L^{-1} trehalose + high temperature stress during filling. FM5: Fanmai 5.

3.11. Quantitative Relationships among Source-Sink-Flow Traits and Yield

To systematically elucidate the coupling relationships among photosynthetic capacity (source), sugar metabolism (flow), dry matter accumulation (sink), and final yield, Redundancy Analysis (RDA) and Partial Least Squares Regression (PLSR) were conducted (**Figure 12**).

The RDA biplot (**Figure 12A**) captured a high proportion of the total variance, with the model explaining 97.0% of the variation (RDA1 = 99.1%). The acute angles between the red arrows (yield and TGW) and the blue arrows (physiological predictor traits) indicated strong positive correlations between the maintenance of physiological activities and yield formation. More importantly, the sample distribution clearly visualized the treatment effects. Heat stress (H) shifted the samples to the far right, in the opposite direction of the yield and physiological vectors, demonstrating severe impairment. In contrast, the application of exogenous TRE, particularly the $T_{15}H$ treatment, markedly shifted the sample clusters back towards the CK along the RDA1 axis. This provides direct multivariate evidence that 15 mmol L^{-1} TRE effectively restored the source-sink-flow balance under heat stress.

To further quantify the relative contributions of these individual traits to yield, Variable Importance in Projection (VIP) scores were extracted from the PLSR model (**Figure 12B**). Variables with a VIP score > 1.0 are considered to have a highly significant driving contribution. The analysis revealed that flag-leaf soluble sugar at 21 DAA (LSS21) had the highest relative contribution (VIP > 1.6), followed by late-stage flag-leaf soluble sugar (LSS28) and photosynthetic parameters. These

quantitative findings confirm that exogenous TRE mitigates heat-induced yield loss primarily by sustaining the "source" carbon assimilation capacity and ensuring the continuous "flow" of soluble sugars during the critical grain-filling windows.

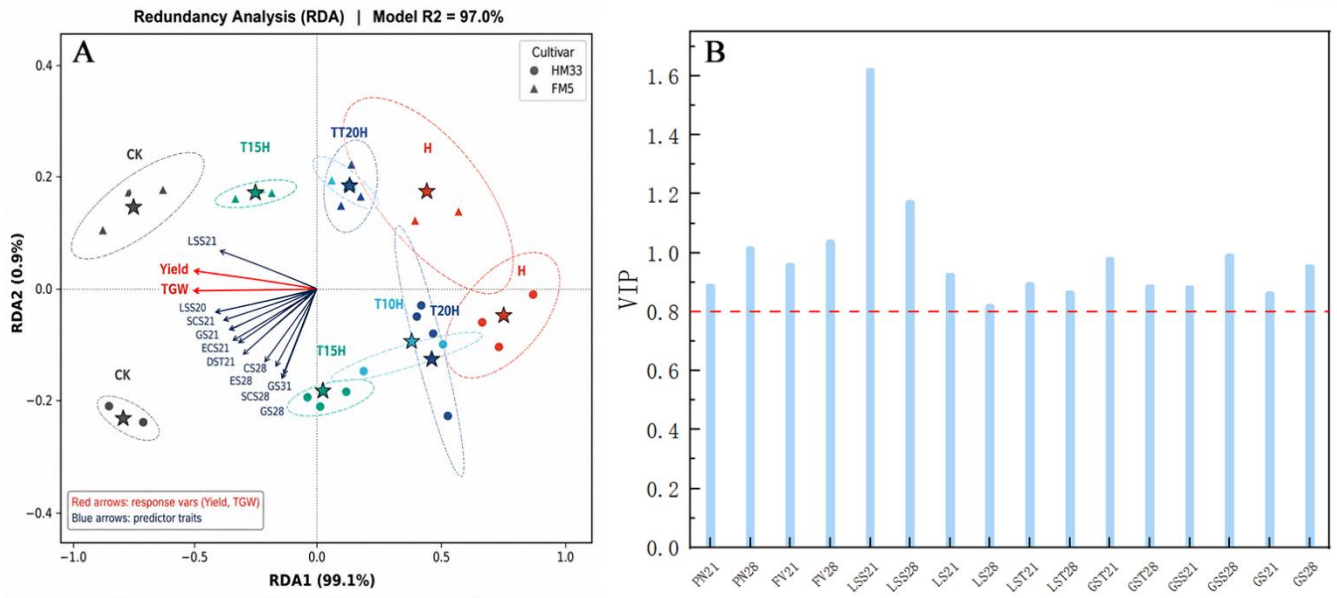

Figure 12. Quantitative relationships among source-sink-flow traits and yield components. Note: (**A**) Redundancy analysis (RDA) biplot showing the multidimensional correlations and treatment separations. Red arrows represent the response variables (Yield and TGW), while blue arrows represent the physiological predictor traits. The angle between arrows indicates the degree of correlation (acute angles represent positive correlations). Points represent individual samples, with shapes indicating different cultivars (circles for HM33, triangles for FM5). Dashed ellipses outline the 95% confidence intervals for each treatment group (CK, H, $T_{10}H$, $T_{15}H$, and $T_{20}H$), and the large stars represent the group centroids. (**B**) Variable Importance in Projection (VIP) scores derived from the Partial Least Squares Regression (PLSR) model. The red dashed line indicates the baseline threshold of VIP = 0.8, and variables with VIP > 1.0 are considered to have a highly significant driving contribution to grain yield. Abbreviations: The numbers 21 and 28 indicate 21 and 28 days after anthesis (DAA), respectively. P_n: net photosynthetic rate (P_n); F_V: maximum photochemical efficiency (F_v/F_m); LSS: leaf soluble sugar; LS: leaf sucrose; LST: leaf starch; GSS: grain soluble sugar; GS: grain sucrose; GST: grain starch; TGW: 1000-grain weight; Yield: grain yield.

4. Discussion

4.1. Exogenous TRE Alleviates Heat-Induced Yield Loss by Stabilizing Grain Weight

In the present study, heat stress during grain filling significantly reduced yield in both wheat varieties, with grain weight identified as the principal factor driving yield loss, consistent with previous reports [53,54] (pp. 1379, pp. 739–749). Heat stress has also been reported to markedly reduce grain weight, thereby further contributing to yield loss [55]. Consistent with these findings, our results further demonstrate that the reduction in grain weight was the principal factor underlying yield loss under heat stress [56] (pp. 823–832). This may be attributed to the high sensitivity of grain filling to temperature fluctuations. Heat stress reduces the number of endosperm cells in developing grains, thereby inhibiting endosperm cell proliferation and decreasing grain sink capacity, i.e., the potential for assimilate accumulation [57] (pp. 729–745).

In our study, both wheat varieties experienced yield reductions under heat stress, though to differing extents, likely reflecting differences in heat tolerance. Notably, the heat-tolerant variety HM33 exhibited a smaller yield decline than the heat-sensitive FM5, potentially due to a stronger post-stress recovery ability, making HM33 less susceptible to heat exposure. Intriguingly, under heat stress, the grain weight reduction across different spikelet positions in HM33 followed the order of upper > lower > middle. This spatial variation is closely related to vascular bundle anatomy and sink priority. The middle spikelets, being physically closer to the major vascular connections of the rachis, experience lower resistance to assimilate transport. Combined with their earlier anthesis, middle spikelets establish a stronger sink demand and temporary priority for carbon partitioning under stress-induced source limitations, resulting in the smallest weight reduction. Evidence from prior work also supports that external interventions to enhance heat resistance can be transformative [58] (pp. 1144). TRE treatment has been shown to significantly increase yield under heat stress [59], which is consistent with our findings. In the present study, TRE application markedly improved wheat yield under heat stress, and foliar application of 15 mmol L^{-1} TRE most effectively alleviated heat stress-induced yield loss during grain filling. Heat stress also significantly reduced dry matter accumulation in different wheat organs, suggesting that heat stress during grain filling impairs yield formation by limiting dry matter accumulation in these organs. This reduction may result from heat-induced damage to photosynthetic organs and excessive accumulation of reactive oxygen species, which inhibit photosynthetic nutrient assimilation and conversion in vegetative organs, such as leaves and stems. In the present study, the heat stress-induced reduction in dry matter at maturity was greater in the heat-sensitive cultivar FM5 than in the heat-tolerant cultivar HM33. The greatest reductions were observed in the upper three leaves, particularly in the second leaf from the top. TRE treatment most effectively alleviated the decline in dry matter accumulation in flag leaves. This finding may be associated with the high susceptibility of chlorophyll contents in the flag leaf and the second leaf from the top to heat stress during grain filling, which can subsequently affect yield-related traits [60] (pp. 317–320). Our results further indicate that the application of 15 mmol L^{-1} TRE at flowering enhanced dry matter accumulation in reproductive organs, thereby alleviating grain weight reduction and subsequent yield loss under heat stress.

4.2. Mitigation of Photosynthetic Degradation and Chloroplast Damage by TRE

Moreover, photosynthetic efficiency has been identified as a key indicator of crop yield [61] (pp. 380–388). Heat stress suppresses plant growth, accelerates chlorophyll degradation, damages the photosynthetic system, induces premature aging of functional leaves, and reduces photosynthetic rate. TRE treatment has been reported to protect the photosynthetic system of wheat seedlings under heat stress [42] (pp. 770–776). In our study, Transmission electron microscopy (TEM) of flag leaves showed that TRE treatment effectively mitigated heat-induced damage. Specifically, TRE application preserved the integrity of cellular and chloroplast membranes, and prevented the deformation of grana lamellae. Ultimately, these protective effects on

the photosynthetic ultrastructure contributed to the enhanced heat tolerance of flag leaves. We also found that TRE treatment significantly improved the net photosynthetic rate (P_n), which might play a role in modulating plant water status, potentially by influencing stomatal behavior or transpiration to sustain photosynthesis under heat stress. However, direct physiological parameters such as stomatal conductance (g_s), transpiration rate (E), and leaf water potential (Ψ_w) were not measured in this study and require further verification. Existing literature shows that heat stress causes stomatal closure, disrupts chloroplast structures, and reduces chlorophyll content [62–64] (pp. 45–55, pp. 143–155). Based on the literature, TRE is widely reported to promote heat shock protein production and enhance antioxidant enzyme activity, thereby reducing heat-induced oxidative damage and stabilizing biological membranes [65] (pp. 1–16). In our study, TRE application effectively maintained chloroplast ultrastructural integrity (**Figure 4**) and improved chlorophyll fluorescence parameters (**Figure 3**), suggesting that TRE helps chloroplasts better capture and utilize light energy. This protective effect, which might be associated with the maintenance of cellular homeostasis under high-temperature stress, collectively contributed to reduced heat damage and improved heat tolerance in wheat flag leaves. Foliar application of TRE at the flowering stage increased the potential photosynthetic capacity and light-use efficiency of flag leaves, thereby maintaining normal photosynthetic function, promoting the formation and translocation of photosynthates, and enhancing dry matter accumulation. These effects ultimately alleviated yield loss under heat stress, with the optimal response observed at 15 mmol L^{-1} TRE. The preservation of chloroplast ultrastructure and the maintenance of higher P_n and F_v/F_m values under heat stress may be attributed to the unique biophysical properties of TRE. As a typical osmoprotectant and chemical chaperone, TRE can replace water molecules on the surfaces of lipid bilayers and proteins, such as Rubisco and the D1 protein of PSII, through hydrogen bonding, thereby preventing heat-induced protein denaturation and membrane fluidization [66] (pp. 417–441). Furthermore, exogenous TRE might alleviate oxidative damage by acting as a signaling molecule to upregulate the activities of ROS-scavenging enzymes, which explains the delayed senescence and sustained photochemical efficiency in flag leaves. Moreover, following TRE application, the heat-sensitive cultivar FM5 exhibited greater recovery of photosynthetic capacity than HM33. This response may be attributable to the weaker inherent stress resistance of FM5, for which exogenous TRE may provide greater protection of the physiological functions of photosynthetic organs.

4.3. Regulation of Sugar Metabolism and Translocation under Heat Stress

Sugars are essential for plant growth, serving not only as energy sources but also as important determinants of plant quality and yield. Sugar metabolism is a fundamental biological process involved in protein composition, lipid degradation, nucleic acid synthesis, and secondary metabolism. In addition to providing energy, sugars function as signaling molecules that regulate plant growth, development, and responses to environmental stimuli. Soluble sugars are major components of plant carbohydrates, and their concentrations reflect the capacity for photosynthetic

assimilation as well as the transport and utilization of photoassimilates; therefore, they are widely regarded as reliable indicators of photosynthetic performance [67] (pp. 388–393). Previous studies have demonstrated that soluble sugar contents increase under stress conditions, thereby alleviating ionic stress, stabilizing cellular structures, and enhancing stress tolerance [68–70] (pp. 89–96, pp. 359). Consistent with these findings, our study showed that appropriate concentrations of exogenous TRE significantly increased soluble sugar contents in flag leaves and grains under heat stress during grain filling. These treatments promoted sugar metabolism, increased endogenous sugar synthesis, enhanced soluble sugar accumulation, improved water uptake, stabilized cellular osmotic potential, and maintained photosynthetic stability, thereby enhancing wheat heat tolerance.

Sucrose is a major carbohydrate source and serves as the primary transport and storage form of assimilated carbon in plants. After flowering, wheat leaves synthesize sucrose and export it to developing grains, where it is cleaved, thereby completing the sucrose metabolic process. Grain development is strongly constrained by photosynthetic capacity. Sucrose synthesis in leaves reflects the development and functional status of “source” organs, whereas sucrose cleavage in grains reflects the development of “sink” organs. Previous studies have suggested that exogenous TRE promotes sugar accumulation, maintains relatively high respiratory activity, reduces starch accumulation in vegetative organs, alleviates photosynthetic feedback inhibition, and facilitates starch partitioning between “source” and “sink” organs. These effects ultimately enhance photosynthesis and assimilate accumulation [71] (pp. 544–567). Mechanistically, the regulation of sugar metabolism by TRE is closely linked to the trehalose-6-phosphate (T6P) signaling pathway. T6P serves as a critical sensor of sucrose status. Exogenous TRE application likely alters the endogenous T6P/sucrose ratio, which subsequently modulates the activity of SnRK1 (sucrose non-fermenting-1-related protein kinase 1), a central master regulator of carbon and energy metabolism [72] (pp. 7–27). This regulatory mechanism is strongly supported by evidence showing that chemical intervention in the T6P-SnRK1 pathway in wheat directly coordinates source-sink relationships, thereby enhancing photosynthetic enzyme activity (such as Rubisco) in source leaves and promoting starch biosynthetic enzymes (such as AGPase) in sink organs, leading to increased grain yield and stress resilience [73] (pp. 574–578). Under heat stress, this T6P-SnRK1 signaling cascade can upregulate the activities of key sucrose-cleaving enzymes (such as invertases and sucrose synthase) in sink organs (grains), while maintaining sucrose-phosphate synthase (SPS) activity in source organs (flag leaves) [74] (pp. 2623–2638). This sustained source-to-sink assimilate flow is consistent with our observation that TRE-treated wheat maintained higher sucrose and starch contents in both flag leaves and developing grains. These results suggest that TRE enhanced photosynthate translocation and starch biosynthesis, which may have contributed to alleviating the heat-induced reduction in 1000-grain weight. In the present study, TRE application at the flowering stage increased sucrose and starch contents in flag leaves and grains, possibly because TRE enhanced sucrose metabolism in source organs and promoted the translocation of photosynthates to sink organs. However, owing to limitations in assimilate transport, sugars produced in flag leaves may not be rapidly loaded into the grains, resulting in starch accumulation in the leaves. Meanwhile, an adequate sucrose

supply and active sucrose cleavage in sink organs supported rapid starch accumulation in the grains. Notably, this physiological enhancement in starch accumulation was structurally supported by the preserved morphology of starch granules (Section 3.10). In the present study, heat stress during grain filling impaired starch granule development, leading to deformed structures and loose packing, which directly restricted the starch accumulation space in the endosperm and led to the observed decrease in 1000-grain weight (**Table 2**). In contrast, the application of 15 mmol L^{-1} TRE effectively protected the structural integrity of both A-type and B-type starch granules and maintained their tight arrangement. This micro-structural preservation facilitated efficient physical packing of starch in endosperm cells, thereby securing grain weight and mitigating final yield loss.

Starch occurs as aggregated granules that are classified into A-, B-, and C-type granules according to their diameter. Compared with early grain filling, heat stress causes a more pronounced decline in the proportion of B-type starch granules during mid-grain filling, whereas the proportion of A-type starch granules shows the opposite trend [75] (pp. 363–375). In the present study, heat stress caused pronounced deformation of all starch granule types and markedly increased surface microporosity, which may alter the internal structure of starch and adversely affect processing quality. These heat stress-induced morphological alterations were partially alleviated by exogenous TRE application, although the underlying mechanisms require further investigation. Nevertheless, TRE application could not fully compensate for the losses induced by high temperature.

Crucially, previous studies have often treated photosynthesis and sugar accumulation as isolated physiological responses. In the present study, by integrating RDA and PLSR models based on the source-sink-flow concept, we quantitatively identified the hierarchical contributions of these traits to yield recovery. Our PLSR analysis confirmed that the relative contribution of flag-leaf soluble sugar (LSS) and late-stage photosynthetic efficiency (F_v/F_m 28, P_n 28) significantly outweighed other parameters (VIP > 1.0). This provides robust statistical evidence that exogenous TRE mitigates heat-induced yield loss not merely by acting as a general osmoprotectant, but specifically by sustaining the “source” carbon assimilation capacity and ensuring the continuous “flow” of soluble sugars from flag leaves to developing grains during critical heat-stress windows. Although our physiological data highlight the prominent role of TRE in sugar allocation, future molecular studies focusing on the transcriptomic profiling of sucrose transporters and the T6P-SnRK1 signaling cascade are required to fully unravel these precise mechanisms. Indeed, our previous physiological and transcriptomic analysis of wheat under temperature warming revealed that temperature shifts drastically regulate candidate genes associated with starch and sucrose metabolism, plant hormone transduction, and carbohydrate biosynthesis [76] (pp. 1044-1064), suggesting a highly complex regulatory network that warrants further molecular investigation under post-anthesis terminal heat stress.

4.4. Study Limitations

In the present study, passive warming plastic sheds were utilized to simulate post-anthesis heat stress during the grain-filling stage of wheat. Although this method

effectively elevated the canopy temperature to evaluate the protective role of exogenous TRE, certain microclimatic limitations exist compared with active open-field warming systems, such as Free-Air Temperature Increase (FATI) infrared arrays. Passive plastic sheds inevitably block natural wind flow, which reduces wind speed inside the canopy, thereby increasing boundary layer resistance on wheat flag leaves and potentially reducing their natural transpiration rates. Furthermore, passive warming sheds may slightly increase relative humidity and alter the solar radiation spectrum reaching the crop canopy due to film filtration. These microclimatic variations can affect the canopy energy balance and source-sink relations differently than under natural, open-field conditions. Therefore, while our study provides valuable physiological, ultrastructural, and biochemical insights, future research utilizing open-field FATI systems is recommended to validate the field-scale agronomic performance and practical application rates of exogenous TRE under natural meteorological conditions.

5. Conclusion

Terminal heat stress during the grain-filling stage significantly reduces winter wheat yield, primarily by decreasing the thousand-grain weight, with the heat-sensitive cultivar (FM5) suffering greater losses than the heat-tolerant cultivar (HM33). Our results demonstrate that foliar application of 15 mmol L^{-1} exogenous trehalose (TRE) at anthesis serves as an effective agronomic strategy to mitigate this heat-induced yield penalty. By integrating physiological data with RDA and PLSR models based on a "source-flow-sink" framework, we quantitatively established the coordinated regulatory pathways of TRE. Specifically, TRE effectively preserves chloroplast ultrastructural integrity and late-stage photosynthetic capacity (source maintenance), ensuring the continuous synthesis and transport of flag-leaf soluble sugars and sucrose (flow efficiency). The PLSR analysis quantitatively identified that the maintenance of flag-leaf soluble sugar at 21 DAA and late-stage photosynthetic performance were the dominant drivers (VIP > 1.0) for yield recovery. This robust assimilate supply ultimately facilitated starch accumulation and grain filling (sink strength). Despite these clear physiological benefits, the present study has certain limitations. The passive plastic warming sheds utilized herein may introduce microclimatic artifacts, such as reduced canopy wind speed and altered relative humidity, compared to natural open-field conditions. Furthermore, the precise molecular regulatory networks require further exploration. Future studies utilizing open-field active warming systems (e.g., FATI) combined with transcriptomic profiling of the T6P-SnRK1 signaling cascade are warranted to fully validate the field-scale performance and elucidate the underlying molecular mechanisms of TRE-mediated heat resilience.

Author contributions: Y.F. Conceptualization, Methodology, Formal Analysis, Visualization, Writing-Original Draft; N.C. Conceptualization, Methodology, Data Curation, Formal Analysis, Visualization, Writing-Original Draft, Writing-Review & Editing; X.Y. Data Curation, Writing-Review & Editing; L.X. Manuscript revision; Y.Y. Data Curation; Y.L. Data Curation; B.L. Data Curation; X.W. Data Curation;

W.Z. Resources; S.M. Resources; Z.Z. Resources; Z.S. Resources; H.Z. Conceptualization, Supervision; D.J. Conceptualization, Supervision; Z.H. (Corresponding Author): Supervision, Methodology, Conceptualization, Resources.

Funding: This work was supported by the National Natural Science Foundation of China (32502034), National Key R&D Program of China (2023YFD2300202), National Natural Science Foundation of China (32372223), National Natural Science Foundation of China (32472232, U19A2021), Anhui Collaborative Innovation Center for Grain Crops, and the Major Science and Technology Special Project of Anhui Province (S202003a06020035).

Acknowledgments: We acknowledge the support from Jiangsu Collaborative Innovation Center for Modern Crop Production (JCIC-MCP).

Conflict of interest: The authors declare that we have no conflicts of interest.

References

1. Tao F., Zhang Z., Zhang S., Rötter R.P. Heat stress impacts on wheat growth and yield were reduced in the Huang-Huai-Hai plain of China in the past three decades. European Journal of Agronomy. 2015, 71, 44–52. https://doi.org/10.1016/j.eja.2015.08.003
2. Li J., Li Z., Li X., Tang X., Liu H., Li J., Song Y. Effects of spraying KH2PO4 on flag leaf physiological characteristics and grain yield and quality under heat stress during the filling period in winter wheat. Plants. 2023, 12, 1801. https://doi.org/10.3390/plants12091801
3. Wu X., Gong D., Zhao K., Chen D., Dong Y., Gao Y., Wang Q., Hao G.F. Research and development trends in plant growth regulators. Advanced Agrochem. 2024, 3, 99–106. https://doi.org/10.1016/j.aac.2023.11.005
4. Sehar Z., Mir T.R., Khan S., Masood A., Khan N.A. Nitric oxide and proline modulate redox homeostasis and photosynthetic metabolism in wheat plants under high temperature stress acclimation. Plants. 2023, 12, 1256. https://doi.org/10.3390/plants12061256
5. Müller J., Aeschbacher R.A., Sprenger N., Boller T., Wiemken A. Disaccharide-mediated regulation of sucrose: Fructan-6-fructosyltransferase, a key enzyme of fructan synthesis in barley leaves. Plant Physiology. 2000, 123, 265–273. https://doi.org/10.1104/pp.123.1.265
6. Vogel G., Fiehn O., Jean-Richard-dit-Bressel L., Boller T., Wiemken A., Aeschbacher R.A., Wingler A. Trehalose metabolism in Arabidopsis: Occurrence of trehalose and molecular cloning and characterization of trehalose-6-phosphate synthase homologues. Journal of Experimental Botany. 2001, 52, 1817–1826. https://doi.org/10.1093/jexbot/52.362.1817
7. Garg A.K., Kim J.K., Owens T.G., Ranwala A.P., Choi Y.D., Kochian L.V., Wu R.J. Trehalose accumulation in rice plants confers high tolerance levels to different abiotic stresses. Proceedings of the National Academy of Sciences. 2002, 99, 15898–15903. https://doi.org/10.1073/pnas.252637799
8. Sadak M.S. Physiological role of trehalose on enhancing wheat plant tolerance to water deficit. Biocatalysis and Agricultural Biotechnology. 2019, 21, 101315. https://doi.org/10.1016/j.bcab.2019.101315
9. Mirosavljević M., Mikić S., Župunski V., Abdelhakim L., Trkulja D., Zhou R., Špika A.K., Ottosen C.O. Effects of heat stress during anthesis and grain filling stages on some physiological and agronomic traits in diverse wheat genotypes. Plants. 2024, 13, 2083. https://doi.org/10.3390/plants13152083
10. Semenov M., Shewry P. Modelling predicts that heat stress and not drought will limit wheat yield in Europe. Nature Precedings. 2010, 1–1. https://doi.org/10.1038/npre.2010.4335.1
11. Stone P.J., Nicolas M.E. Effect of timing of heat stress during grain filling on two wheat varieties differing in heat tolerance. II. Fractional protein accumulation. Australian Journal of Plant Physiology. 1996, 23, 739–749. https://doi.org/10.1071/pp9960739
12. Riaz-ud-Din M. S., Subhani G.M., Ahmad N., Hussain M., Rehman A.U. Effect of temperature on development and grain formation in spring wheat. Pakistan Journal of Botany. 2010, 42, 899–906.

13. Bita C.E., Gerats T. Plant tolerance to high temperature in a changing environment: Scientific fundamentals and production of heat stress-tolerant crops. Frontiers in Plant Science. 2013, 4, 273. https://doi.org/10.3389/fpls.2013.00273
14. Shao R., Yu K., Li H., Jia S., Yang Q., Zhao X., Zhao Y., Liu T. The effect of elevating temperature on the growth and development of reproductive organs and yield of summer maize. Journal of Integrative Agriculture. 2021, 20, 1783–1795. https://doi.org/10.1016/S2095-3119(20)63304-4
15. Zhao K., Tao Y., Liu M., Yang D., Zhu M., Ding J., Zhu X., Guo W., Zhou G., Li C. Does temporary heat stress or low temperature stress similarly affect yield, starch, and protein of winter wheat grain during grain filling? Journal of Cereal Science. 2022, 103, 103408. https://doi.org/10.1016/j.jcs.2021.103408
16. Singh S.K., Barman M., Prasad J.P., Bahuguna R.N. Phenotyping diverse wheat genotypes under terminal heat stress reveal canopy temperature as critical determinant of grain yield. Plant Physiology Reports. 2022, 27, 335–344. https://doi.org/10.1007/s40502-022-00647-y
17. Zhao Y., Wang X., Wang J., Fu X., Dong Z., Shi Z., Guo J., He M. Effects of heat stress on grain-filling rate of different wheat varieties. Chinese Journal of Eco-Agriculture. 2016, 24, 1239–1245. https://doi.org/10.13930/j.cnki.cjea.160056
18. Chen G., Li K., Gu H., Cheng Y., Xue D., Jia H., Du Z., Li Z. Climatic challenges in the growth cycle of winter wheat in the Huang-Huai-Hai plain: New perspectives on high-temperature–drought and low-temperature–drought compound events. Atmosphere. 2024, 15, 747. https://doi.org/10.3390/atmos15070747
19. Correia P.M.P., da Silva A.B., Roitsch T., Carmo-Silva E., Marques da Silva J. Photoprotection and optimization of sucrose usage contribute to faster recovery of photosynthesis after water deficit at high temperatures in wheat. Physiologia Plantarum. 2021, 172, 615–628. https://doi.org/10.1111/ppl.13227
20. Djanaguiraman M., Narayanan S., Erdayani E., Prasad P.V.V. Effects of high temperature stress during anthesis and grain filling periods on photosynthesis, lipids and grain yield in wheat. BMC Plant Biology. 2020, 20, 268. https://doi.org/10.1186/s12870-020-02479-0
21. Ancín M., Gámez A.L., Jauregui I., Galmes J., Sharwood R.E., Erice G., Ainsworth E.A., Tissue D.T., Sanz-Sáez A., Aranjuelo I. Does the response of rubisco and photosynthesis to elevated [CO2] change with unfavourable environmental conditions? Journal of Experimental Botany. 2024, 75, 7351–7364. https://doi.org/10.1093/jxb/erae379
22. Wang J., Han Y., Li H., Bai H., Liang H., Zong Y., Zhang D., Shi X., Li P., Hao X. Elevated CO_2 concentration extends reproductive growth period and enhances carbon metabolism in wheat exposed to increased temperature. Plant, Cell and Environment. 2025, 48, 1452–1467. https://doi.org/10.1111/pce.15243
23. Talukder A.S.M.H.M., McDonald G.K., Gill G.S. Effect of short-term heat stress prior to flowering and at early grain set on the utilization of water-soluble carbohydrate by wheat genotypes. Field Crops Research. 2013, 147, 1–11. https://doi.org/10.1016/j.fcr.2013.03.013
24. Liu B., Asseng S., Wang A., Wang S., Tang L., Cao W., Zhu Y., Liu L. Modelling the effects of post-heading heat stress on biomass growth of winter wheat. Agricultural and Forest Meteorology. 2017, 247, 476–490. https://doi.org/10.1016/j.agrformet.2017.08.018
25. Maity S., Shrivastav S.P. Understanding heat stress and tolerance mechanisms in wheat (Triticum aestivum L.): A comprehensive review. Journal of Advances in Biology & Biotechnology. 2024, 27, 1196–1211. https://doi.org/10.9734/jabb/2024/v27i71079
26. Farooq M., Bramley H., Palta J.A., Siddique K.H.M. Heat stress in wheat during reproductive and grain-filling phases. Critical Reviews in Plant Sciences. 2011, 30, 491–507. http://doi.org/10.1080/07352689.2011.615687
27. Filaček A., Živčák M., Ferroni L., Barboričová M., Gašparovič K., Yang X., Landi M., Brestič M. Pre-acclimation to elevated temperature stabilizes the activity of photosystem I in wheat plants exposed to an episode of severe heat stress. Plants. 2022, 11, 616. https://doi.org/10.3390/plants11050616
28. Dai H., Zhang P., Lu C., Jia G., Song H., Ren X., Chen J., Wei A., Feng B., Zhang S. Leaf senescence and reactive oxygen species metabolism of broomcorn millet (Panicum miliaceum L.) under drought condition. Australian Journal of Crop Science. 2011, 5, 1655–1660. https://doi.org/10.3316/informit.006119856777700
29. Wang X., Cai J., Liu F., Dai T., Cao W., Wollenweber B., Jiang D. Multiple heat priming enhances thermo-tolerance to a later high temperature stress via improving subcellular antioxidant activities in wheat seedlings. Plant Physiology and Biochemistry. 2014, 74, 185–192. https://doi.org/10.1016/j.plaphy.2013.11.014

30. Zhang J., Tan D.K.Y., Shaghaleh H., Chang T., Alhaj Hamoud Y. Response of photosynthesis in wheat (triticum aestivum L.) cultivars to moderate heat stress at meiosis and anthesis stages. Agronomy. 2023, 13, 2251. https://doi.org/10.3390/agronomy13092251
31. Farrar J., Pollock C., Gallagher J. Sucrose and the integration of metabolism in vascular plants. Plant Science. 2000, 154, 1–11. https://doi.org/10.1016/S0168-9452(99)00260-5
32. Göbel M., Fichtner F. Functions of sucrose and trehalose 6-phosphate in controlling plant development. Journal of Plant Physiology. 2023, 291, 154140. https://doi.org/10.1016/j.jplph.2023.154140
33. Liu H., Li T., Hou J., Yin X., Wang Y., Si X., Rehman S.U., Zhuang L., Guo W., Hao C., Zhang X. TaWUS-like-5D affects grain weight and filling by inhibiting the expression of sucrose and trehalose metabolism-related genes in wheat grain endosperm. Plant Biotechnology Journal. 2025, 23, 2018–2033. https://doi.org/10.1111/pbi.70015
34. Stitt M., Huber S., Kerr P. 6 - control of photosynthetic sucrose formation. In: Hatch M.D., Boardman N.K. (editors). Photosynthesis, Academic Press: Cambridge, MA, USA, 1987. 10, pp. 327–409. https://doi.org/10.1016/B978-0-12-675410-0.50012-9
35. Lalonde S., Tegeder M., Throne-Holst M., Frommer W.B., Patrick J.W. Phloem loading and unloading of sugars and amino acids. Plant, Cell and Environment. 2003, 26, 37–56. https://doi.org/10.1046/j.1365-3040.2003.00847.x
36. Keeling P.L., Wood J.R., Tyson R.H., Bridges I.G. Starch biosynthesis in developing wheat grain 1: Evidence against the direct involvement of triose phosphates in the metabolic pathway. Plant Physiology.1988, 87, 311–319. https://doi.org/10.1104/pp.87.2.311
37. Gao H., Niu J., Zhao W., Zhang D., Li S., Xu Y., Liu Y. The effect and regulation mechanism of powdery mildew on wheat grain carbon metabolism. Starch-Stärke. 2022, 74, 2100239. https://doi.org/10.1002/star.202100239
38. Du L., Li S., Ding L., et al. Genome-wide analysis of trehalose-6-phosphate phosphatases (TPP) gene family in wheat indicates their roles in plant development and stress response. BMC Plant Biology. 2022, 22, 120. https://doi.org/10.1186/s12870-022-03504-0
39. Paul M.J., Sahu P.P., Puranik S., Griffiths C.A. Trehalose 6-phosphate and hormone signalling crosstalk. Current Opinion in Plant Biology. 2026, 92, 102921. https://doi.org/10.1016/j.pbi.2026.102921
40. Luo Y., Wang Y., Xie Y., et al. Transcriptomic and Metabolomic Analyses of the Effects of Exogenous Trehalose on Heat Tolerance in Wheat. International Journal of Molecular Sciences. 2022, 23, 5194. https://doi.org/10.3390/ijms23095194
41. Luo Y., Wang W., Fan Y.Z., et al. Exogenously-Supplied Trehalose Provides Better Protection for D1 Protein in Winter Wheat under Heat Stress. Russian Journal of Plant Physiology. 2018, 65, 115–122. https://doi.org/10.1134/S1021443718010168
42. Luo Y., Xie Y., He D., et al. Exogenous trehalose protects photosystem II by promoting cyclic electron flow under heat and drought stresses in winter wheat. Plant Biology. 2021, 23, 770–776. https://doi.org/10.1111/plb.13277
43. Elkelish A., Alqudah A.M., Alhudhaibi A.M., et al. Framework-primed trehalose: fast-tracking abiotic stress memory. Plant Cell Reports. 2026, 45, 15. https://doi.org/10.1007/s00299-025-03685-6
44. Li Y., Ma L., Zhang Y., et al. Effects of exogenous trehalose on flag leaf physiological traits and yield of wheat under heat stress during grain filling. Acta Agronomica Sinica (China). 2023, 49, 2210–2224. https://doi.org/10.3724/SP.J.1006.2023.21057
45. Luo Y., Gao Y., Wang W., Zou C. Application of trehalose ameliorates heat stress and promotes recovery of winter wheat seedlings. Biologia Plantarum. 2014, 58, 395–398. https://doi.org/10.1007/s10535-014-0397-6
46. Sadak M.S. Physiological role of trehalose on enhancing salinity tolerance of wheat plant. Bulletin of the National Research Centre. 2019, 43, 1–10. https://doi.org/10.1186/s42269-019-0098-6
47. Zhao D., Li T., Hao Z., Cheng M., Tao J. Exogenous trehalose confers high temperature stress tolerance to herbaceous peony by enhancing antioxidant systems, activating photosynthesis, and protecting cell structure. Cell Stress and Chaperones. 2019, 24, 247–257. https://doi.org/10.1007/s12192-018-00961-1
48. Zhang X., Liu Y., Wang Z., Chen D., Ren L. Effects of sowing date and density on dry matter accumulation, translocation and yield of Ningfengmai No. 6. Journal of Zhejiang Agricultural Sciences. 2025, 1–15. https://doi.org/10.16178/j.issn.0528-9017.20250923 (in Chinese)
49. Genty B., Briantais J.M., Baker N.R. The relationship between the quantum yield of photosynthetic electron transport and quenching of chlorophyll fluorescence. Biochimica et Biophysica Acta (BBA) - General Subjects. 1989, 990, 87–92. https://doi.org/10.1016/S0304-4165(89)80016-9 (in Chinese)

50. Jia W., Zhang J. Stomatal movements and long-distance signaling in plants. Plant Signaling & Behavior. 2008, 3, 772–777. https://doi.org/10.4161/psb.3.10.6294
51. Li H. Principles and Techniques of Plant Physiological and Biochemical Experiment. Higher Education Press: Beijing, China, 2000. pp. 60–70 (in Chinese)
52. Guo D., Peng X. Comparative study on two determination methods of starch by anthrone colorimetry and enzymatic hydrolysis. Journal of Hunan University of Arts and Science (Natural Science Edition). 2007, 19, 34–36. https://doi.org/10.3969/j.issn.1672-6164.2007.03.011 (in Chinese)
53. Yang J., Feng Y., Chi T., Wen Q., Liang P., Wang A., Li P. Mitigation of elevated CO_2 concentration on warming-induced changes in wheat is limited under extreme temperature during the grain filling period. Agronomy. 2023, 13, 1379. https://doi.org/10.3390/agronomy13051379
54. Stone P.J., Nicolas M.E. Effect of timing of heat stress during grain filling on two wheat varieties differing in heat tolerance. II. Fractional protein accumulation. Australian Journal of Plant Physiology. 1996, 23, 739–749. https://doi.org/10.1071/pp9960739
55. Groli E.L., Frascaroli E., Maccaferri M., Ammar K., Tuberosa R. Dissecting the effect of heat stress on durum wheat under field conditions. Frontiers in Plant Science. 2024, 15, 1393349. https://doi.org/10.3389/fpls.2024.1393349
56. Mirosavljević M., Mikić S., Župunski V., Kondić Špika A., Trkulja D., Ottosen C.O., Zhou R., Abdelhakim L. Effects of high temperature during anthesis and grain filling on physiological characteristics of winter wheat cultivars. Journal of Agronomy and Crop Science. 2021, 207, 823–832. https://doi.org/10.1111/jac.12546
57. Harris P.J., Burrell M.M., Emes M.J., Tetlow I.J. Effects of post-anthesis high-temperature stress on carbon partitioning and starch biosynthesis in a spring wheat (triticum aestivum L.) adapted to moderate growth temperatures. Plant and Cell Physiology. 2023, 64, 729–745. https://doi.org/10.1093/pcp/pcad030
58. Cao L., Fahim A.M., Liang X., Fan S., Song Y., Liu H., Ye F., Ma C., Zhang D., Lu X. Melatonin enhances heat tolerance via increasing antioxidant enzyme activities and osmotic regulatory substances by upregulating zmeno1 expression in maize (zea mays L.). Antioxidants. 2024, 13, 1144. https://doi.org/10.3390/antiox13091144
59. Luo Y., Liu X., Li W. Exogenously-supplied trehalose inhibits the growth of wheat seedlings under high temperature by affecting plant hormone levels and cell cycle processes. Plant Signaling and Behavior. 2021, 16, 1907043. https://doi.org/10.1080/15592324.2021.1907043
60. Xu X., Zhang Y., Wang Z. Effect of heat stress during grain filling on phosphoenolpyruvate carboxylase and ribulose-1,5-bisphosphate carboxylase/oxygenase activities of various green organs in winter wheat. Photosynthetica. 2004, 42, 317–320. https://doi.org/10.1023/B:PHOT.0000040608.97976.a3
61. Wu A., Hammer G.L., Doherty A., von Caemmerer S., Farquhar G.D. Quantifying impacts of enhancing photosynthesis on crop yield. Nature Plants. 2019, 5, 380–388. https://doi.org/10.1038/s41477-019-0398-8
62. Chen Y., Zhang C., Su Y., Ma J., Zhang Z., Yuan M., Zhang H., Yuan S. Responses of photosystem II and antioxidative systems to high light and high temperature co-stress in wheat. Environmental and Experimental Botany. 2017, 135, 45–55. https://doi.org/10.1016/j.envexpbot.2016.12.001
63. Feng B., Liu P., Li G., Dong S., Wang F., Kong L., Zhang J. Effect of heat stress on the photosynthetic characteristics in flag leaves at the grain-filling stage of different heat-resistant winter wheat varieties. Journal of Agronomy and Crop Science. 2014, 200, 143–155. https://doi.org/10.1111/jac.12045
64. Hu S., Ding Y., Zhu C. Sensitivity and responses of chloroplasts to heat stress in plants. Frontiers in Plant Science. 2020, 11. 375. https://doi.org/10.3389/fpls.2020.00375
65. Raza A., Bhardwaj S., Atikur Rahman M., García-Caparrós P., Habib M., Saeed F., Charagh S., Foyer C.H., Siddique K.H.M., Varshney R.K. Trehalose: A sugar molecule involved in temperature stress management in plants. The Crop Journal. 2024, 12, 1–16. https://doi.org/10.1016/j.cj.2023.09.010
66. Paul M.J., Primavesi L.F., Jhurreea D., Zhang Y. Trehalose Metabolism and Signaling. Annual Review of Plant Biology. 2008, 59, 417–441. https://doi.org/10.1146/annurev.arplant.59.032607.092945
67. Rosa M., Prado C., Podazza G., Interdonato R., González J.A., Hilal M., Prado F.M. Soluble sugars: Metabolism, sensing and abiotic stress: a complex network in the life of plants. Plant Signaling and Behavior. 2009, 4, 388–393. https://doi.org/10.4161/psb.4.5.8294
68. Khan N., et al. Role of sugars, amino acids and organic acids in improving plant abiotic stress tolerance. Pakistan Journal of Botany. 2020, 52(2), 355–363. https://doi.org/10.30848/PJB2020-2(24)

69. Redillas M.C.F.R., Park S.H., Lee J.W., Kim Y.S., Jeong J.S, Jung H., Bang S.W., Hahn T.R., Kim J.K Accumulation of trehalose increases soluble sugar contents in rice plants conferring tolerance to drought and salt stress. Plant Biotechnology Reports. 2012, 6, 89–96. https://doi.org/10.1007/s11816-011-0210-3
70. Yang X., Liu R., Jing M., Zhang N., Liu C., Yan J. Variation of root soluble sugar and starch response to drought stress in foxtail millet. Agronomy. 2023, 13, 359. https://doi.org/10.3390/agronomy13020359
71. Lunn J.E., Delorge I., Figueroa C.M., Van Dijck P., Stitt M. Trehalose metabolism in plants, The Plant Journal. 2014, 79, 544–567. https://doi.org/10.1111/tpj.12509
72. Figueroa C.M., Lunn J.E. A Tale of Two Sugars: Trehalose 6-Phosphate and Sucrose. Plant Physiology. 2016, 172. 7–27. https://doi.org/10.1104/pp.16.00417
73. Griffiths C.A., Sagar R., Geng Y., et al. Chemical intervention in plant sugar signalling increases yield and resilience. Nature. 2016, 540, 574–578. https://doi.org/10.1038/nature20591
74. Oszvald M., Primavesi L.F., Griffiths C.A., Cohn J., Basu S.S., Nuccio M.L., M.J. Paul M.J. Trehalose 6-Phosphate Regulates Photosynthesis and Assimilate Partitioning in Reproductive Tissue. Plant Physiology. 2018, 176, 2623–2638. https://doi.org/10.1104/pp.17.01673
75. Bhullar S.S., Jenner C.F. Differential responses to high temperatures of starch and nitrogen accumulation in the grain of four cultivars of wheat. Australian Journal of Plant Physiology. 1985, 12, 363–375. https://doi.org/10.1071/pp9850363
76. Fan Y., Zhang Y., Tang Y., Xie B., He W., Cui G., Yang J., Zhang W., Ma S., Ma C., Zhang H., Huang Z. Response of wheat to winter night warming based on physiological and transcriptome analyses. Journal of Integrative Agriculture. 2025, 24, 1044–1064. https://doi.org/10.1016/j.jia.2024.04.016